THESIS FOR THE DEGREE OF DOCTOR OF PHILOSOPHY

Electrically Conducting Cellulose Yarns for Electronic Textiles

SOZAN DARABI

Department of Chemistry and Chemical Engineering

CHALMERS UNIVERSITY OF TECHNOLOGY

Gothenburg, Sweden 2023

Electrically Conducting Cellulose Yarns for Electronic Textiles
SOZAN DARABI
ISBN 978-91-7905-789-3

Doktorsavhandlingar vid Chalmers tekniska högskola
Ny serie nr 5255
ISSN 0346-718X

Department of Chemistry and Chemical Engineering
Chalmers University of Technology
SE-412 96 Gothenburg
Sweden
Telephone + 46 (0)31-772 1000

Cover:
Photograph of Conducting Cellulose Yarns for Machine-Sewn Electronic Textiles.
(Photographer Anna-Lena Lundqvist/Chalmers)

Chalmers Digitaltryck
Gothenburg, Sweden 2023

Electrically Conducting Cellulose Yarns for Electronic Textiles

Sozan Darabi
Department of Chemistry and Chemical Engineering
Chalmers University of Technology

ABSTRACT

Wearable electronics can be used for the purpose of fitness tracking, health monitoring, energy harvesting, and even for communication. Electronic textiles (e-textiles) are a versatile platform which can be employed for the realization of wearable electronics. E-textiles present an opportunity to incorporate electronics into textiles while also maintaining the feel and wearability of textile materials. To fabricate e-textile devices, electrically conducting yarns can be used as building blocks. It is of importance to use materials that are lightweight, benign, and scalable to enable the widespread use of e-textiles. Electrically conducting yarn can be produced by combining conducting, semiconducting and insulating materials. For energy harvesting applications, textile thermoelectric generators are of interest since these can utilize the temperature gradient between the body and the ambient surroundings to generate electrical energy.

This thesis discusses several strategies for the development of electrically conducting yarns, which were based on conducting polymers and regenerated cellulose yarns. Hole- and electron-transporting conducting polymer-based yarns were realized for the fabrication of textile thermoelectric generators. Various methods to characterize conducting yarns were explored to evaluate properties of interest for e-textile devices, such as procedures for measuring the electrical resistance and the Seebeck coefficient of the yarns. Furthermore, the electrical stability of the yarns was investigated upon washing and bending, to assess if the produced yarns could withstand textile processing and use. Several p-type polymer-based yarns were produced. P-type polymer-based coated cellulose yarns that were generated through a roll-to-roll process showed a record-high bulk conductivity of 36 S cm^{-1} for cellulose based conducting yarn. The durability was demonstrated by machine sewing the yarns into a substrate fabric for thermoelectric device fabrication. Furthermore, this thesis introduces the first example of n-type polymer-based yarns, which were produced by spray-coating regenerated cellulose yarns. The p-type and n-type polymer-based coated cellulose yarns enabled the fabrication of an all polymer-based thermoelectric textile device.

The presented methods are scalable and resulted in conducting yarns with resilient electrical properties that could be used for the fabrication of e-textile devices. The demonstrated conducting polymer-based yarns present new opportunities for further development of textile polymer-based thermoelectric generators.

keywords: conjugated polymers, textiles, electrical properties, regenerated cellulose yarns, electrically conducting yarns, organic thermoelectrics, electronic textiles

PUBLICATIONS

This thesis consists of an extended summery of the following appended papers:

Paper I **Green Conducting Cellulose Yarns for Machine-Sewn Electronic Textiles**
Sozan Darabi, Michael Hummel, Sami Rantasalo, Marja Rissanen, Ingrid Öberg Månsson, Haike Hilke, Byungil Hwang, Mikael Skrifvars, Mahiar M. Hamedi, Herbert Sixta, Anja Lund, and Christian Müller
ACS Appl. Mater. Interfaces, 2020, 12, 56403-56412.
https://doi.org/10.1021/acsami.0c15399

Paper II **A Polymer-Based Textile Thermoelectric Generator for Wearable Energy Harvesting**
Anja Lund, Yuan Tian, Sozan Darabi and Christian Müller
J. Power Sources, 2020, 480, 228836.
https://doi.org/10.1016/j.jpowsour.2020.228836

Paper III **Machine-Washable Conductive Silk Yarns with a Composite Coating of Ag Nanowires and PEDOT:PSS**
Byungil Hwang, Anja Lund, Yuan Tian, Sozan Darabi, and Christian Müller
ACS Appl. Mater. Interfaces, 2020, 12, 27537-27544.
https://doi.org/10.1021/acsami.0c04316

Paper IV **A Polymer-Based n-Type Yarn for Organic Thermoelectric Textiles**
Sozan Darabi, Chi-Yuan Yang, Zerui Li, Jun-Da Huang, Michael Hummel, Herbert Sixta, Simone Fabiano, Christian Müller
Adv. Electron. Mater, 2023
(accepted manuscript)

Paper V **Reinforcing of a Polar Polythiophene with Cellulose Nanofibrils**
Mariza Mone, Sozan Darabi, Sepideh Zokaei, Mariavittoria Craighero, Lovisa Karlsson, Renee Kroon, Christian Müller
(manuscript in preparation)

CONTRIBUTION REPORT

Paper I Main author. Planned the experiments with A.L. and C.M. Assisted I.Ö.M with the OECT sample preparation and data collection. The laundering of prepared samples was done by A.L. and Anders Mårtensson assisted with SEM. Performed all other sample preparation and data collection, which included mechanical and electrical characterization, optical microscopy, thermoelectric device manufacturing and characterization. Was responsible for data analysis, interpretation and wrote the main part of the paper with A.L. and C.M.

Paper II Co-author. Developed the method for manufacturing the conducting yarn. Supervised the manufacturing, electrical and Seebeck characterization of the yarn. Revised the manuscript together with all co-authors.

Paper III Co-author. Developed the method for the pre-treatment of the yarn and the final coating layer of the two coating steps. Performed Seebeck characterization of the conducting yarns. Revised the manuscript together with all co-authors.

Paper IV Main author. Planned the experiments with C.M. Spray-coated yarns and performed electrical characterization of thin films together with C.-Y.Y. and J.-D.H. Anders Mårtensson assisted with SEM. Responsible for sample preparation and data collection from electrical characterization, optical microscopy, and textile device fabrication. The device characterization was performed together with Z.L. Was responsible for data analysis, interpretation and wrote the paper with C.M.

Paper V Co-author. Carried out spectroscopy, mechanical and electrical characterization of films together with M.M. Developed the method for preparation of the conducting yarns. Produced conducting yarns, performed electrical characterization, bending tests of the yarns and optical microscopy with M.M. Assisted with data analysis.

RELATED PUBLICATIONS NOT INCLUDED IN THIS THESIS

Paper VI **Roll-to-Roll Dyed Conducting Silk Yarns: A Versatile Material for E-Textile Devices**
Anja Lund, Sozan Darabi, Sandra Hultmark, Jason D. Ryan, Barbro Andersson, Anna Ström, Christian Müller
Adv. Mater. Technol, 2018, 3, 1800251.
https://doi.org/10.1002/admt.201800251

Paper VII **Robust PEDOT:PSS Wet-Spun Fibers for Thermoelectric Textiles**
Youngseok Kim, Anja Lund, Hyebin Noh, Anna I. Hofmann, Mariavittoria Craighero, Sozan Darabi, Sepideh Zokaei, Jae Il Park, Myung-Han Yoon, Christian Müller
Macromol. Mater. Eng, 2020, 305, 1900749.
https://doi.org/10.1002/mame.201900749

For my loving family

NOMENCLATURE

Symbols and Abbreviations

α	Seebeck coefficient
ΔT	temperature difference
ΔV	voltage difference
κ	thermal conductivity
μ	charge carrier mobility
ρ	electrical resistivity
σ	conductivity
A	cross-sectional area
E_g	bandgap
HOMO	highest occupied molecular orbital
I	current
I_{load}	load current
I_{sd}	source-drain current
K_h	contact resistance between the textile and hot reservoir
K_t	contact resistance between the textile and cold reservoir
K_{tp}	thermal resistance of the thermopile
L	length
LUMO	lowest unoccupied molecular orbital
n	charge carrier concentration
N	number of thermocouples

OECT	organic electrochemical transistor
P_{max}	maximum power
q	electric charge of the charge carrier
R2R	roll-to-roll
R	electrical resistance
R_c	electrical contact resistance
R_{int}	internal resistance
R_{load}	load resistance
T	temperature
T_g	glass transition temperature
V	voltage
V_g	gate voltage
V_{oc}	open-circuit voltage
$V_{oc,max}$	ideal open circuit voltage
V_{sd}	source-drain voltage
ZT	figure of merit

Chemicals

Ag nanowire	silver nanowire
BBL	poly(benzimidazobenzophenanthroline)
BBL:PEI	poly(benzimidazobenzophenanthroline):poly(ethyleneimine)
Bi_2Te_3	bismuth telluride
BNC	bacterial nanocellulose
CNC	cellulose nanocrystals
CNF	cellulose nanofibrils
CNT	carbon nanotubes
CS_2	carbon disulfide
[DBNH][OAc]	1,5-diazabicyclo[4.3.0]-non-5-enium acetate
DMF	dimethylformamide
DMSO	dimethyl sulfoxide
EDOT	3,4-ethylenedioxythiophene
EG	ethylene glycol
F_4TCNQ	2,3,5,6-tetrafluoro-7,7,8,8-tetracyanoquinodimethane
MWCNT	multi-walled carbon nanotubes
$Na_2S_2O_8$	sodium peroxodisulfate
NMMO	*N*-methylmorpholine *N*-oxide
PAN	polyacrylonitrile
PCBM	[6,6]-phenyl-C_{61}-butyric acid methyl ester
PEDOT	poly(3,4-ethylenedioxythiophene)

PEDOT:PSS	poly(3,4-ethylenedioxythiophene):poly(styrene sulfonate)
PEI	poly(ethyleneimine)
p($g_4$2T-T)	polythiophene with tetraethylene glycol side chains
PSS	poly(styrene sulfonate)
SIS	polystyrene-*b*-polyisoprene-*b*-polystyrene
TEMPO	2,2,6,6-tetramethylpiperidine-1-oxyl

TABLE OF CONTENTS

1. Introduction

1.1. Introduction to E-textiles

The interaction with textile materials is pervasive throughout one's day-to-day life. Carpets, sheets, and clothes are only some of the textiles that can be found in households. How we interact with textiles has the potential to change with the addition of electronic functionality to textiles. These electronic textiles (e-textiles) are a versatile platform for the implementation of wearable electronics. E-textiles should incorporate electronics without unduly compromising the feel and appearance of textile materials. One type of wearable device is a textile-based thermoelectric generator, which can be used for energy harvesting. Wearable devices can also be used for health monitoring[1] and communication.[2] The intention with e-textiles is that they should have the capability to connect to –and thus become part of– the *Internet of Things*, which is the network of interconnected small devices.[3] Within the *Internet of Things*, the purpose of e-textiles may be to collect, process, store, and transmit information.[4] The user could wear a garment that would be capable of collecting vital signs, such as pulse[5] and skin temperature,[6] with the ambition of passing on this information to healthcare professionals for diagnostics, monitoring, and treatment planning.[7-9] E-textile health monitoring devices that can remotely track vital signs could aid people that have difficulties accessing health services, such as elderly individuals with limited mobility or people living in rural areas that lack public transportation.

To create e-textiles with intricate patterns, a myriad of methods such as weaving, knitting, and sewing can be used, many of which require electrically conducting fibers and yarns as basic building blocks.[8] Conducting fibers and yarns can be produced through several methods, for example, by adding a conducting component to the material that is used for fiber spinning or by coating an existing fiber/yarn with a conducting material.[4]

Many inorganic semiconducting materials contain scarce and in some cases harmful elements, like gallium, indium, and lead.[10, 11] It is thus important to explore *green electronics*, which are alternative electronics that are based on non-toxic and renewable materials.[10, 12] One promising alternative are organic semiconductors including conjugated polymers, which are based on abundant elements, can display mechanical flexibility, are lightweight and in some cases biocompatible.[10, 13] Conjugated polymers can conduct both ions and electrons, which equips this type of material with unique advantages when creating a variety of e-textile devices that can be used for bioelectronic and thermoelectric applications.[8, 14] Bio-based materials such as cellulose and its derivatives are widely considered for employment as substrates to support electronic components since cellulose is a renewable and non-toxic resource.[15, 16] Regenerated cellulose yarn is thus an interesting material for e-textile fabrication since these are derived from natural sources.[17, 18] The Ioncell-F process, which can be used to produce regenerated cellulose yarn, allows for a variety of feedstocks.[19, 20]

One of the most widely studied conjugated polymers, poly(3,4-ethylenedioxythiophene) (PEDOT), can be processed as an aqueous dispersion when complexed with poly(styrene sulfonate) (PSS; see Figure 1.1 for chemical structures).[21, 22] PEDOT:PSS displays a high degree of ambient stability,[22] can reach a high electrical conductivity of more than 4000 S cm^{-1} upon sulfuric acid post-treatment[23] and features a promising level of biocompatibility, [12, 24] which makes it an interesting material for wearable devices that could be in close contact with the body.

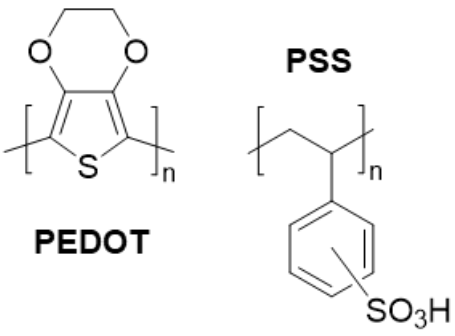

Figure 1.1. Chemical structures of PEDOT and PSS

While hole-transporting (p-type) conducting materials such as PEDOT:PSS have been used to produce electrically conducting yarns,[25] there is a lack of yarns based on electron-transporting (n-type) conducting polymers, likely due to insufficient air-stability of n-type conductors. Recently, an n-type conducting material comprising the conjugated polymer poly(benzimidazobenzophenanthroline) (BBL) and poly(ethyleneimine) (PEI) has been reported (see Figure 1.2 for chemical structures), which features a promising degree of air-stability.[26] Hence, the possibility now exists to develop n-type yarns based on BBL:PEI, which would facilitate the design of, e.g., textile thermoelectric devices, which require both p- and n-type materials.

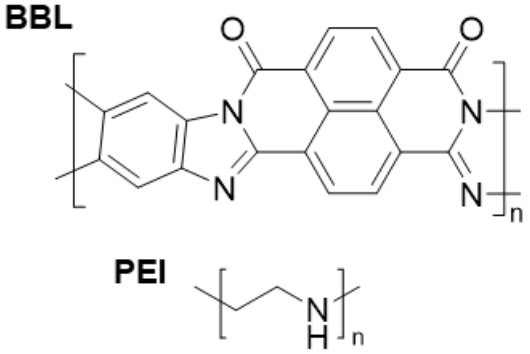

Figure 1.2. Chemical structures of BBL and PEI.

This thesis will explore several strategies for creating electrically conducting yarns that can be used for e-textile manufacturing. An examination of material properties will be followed by the fabrication of prototype devices.

1.2. Aims of the Thesis

The objective of this thesis was to develop electrically conducting yarns based on regenerated cellulose and conducting polymers for the fabrication of e-textile devices. Further, the electrical and electrochemical properties should be suitable for applications such as thermoelectric textile devices and yarn based electrochemical transistors. The ambition was thus to produce both n-type and p-type yarns for the manufacturing of a polymer-based textile thermoelectric generator. Additionally, the conducting yarns were required to feature a high degree of electrical resilience to be able to withstand common textile processing methods as well as durability upon usage and washing. The goal was to create e-textile prototypes to illustrate the various properties of the developed conducting yarns.

2. Textile Fibers

Textile fibers are categorized into natural and man-made fibers (Figure 2.1). Natural fibers can be divided into cellulosic, protein, and mineral fibers. Cellulose-based fibers can be produced from different plants. Cotton, flax and hemp are some examples of cellulosic fibers. Protein-based fibers such as silk and wool are produced by animals. Man-made fibers can be synthetic or regenerated. Synthetic fibers are mostly fabricated from non-renewable resources and poly(ethylene terephthalate) is one of the dominating synthetic fibers. Regenerated fibers are produced from natural sources or cellulose waste streams through chemical processing.[17, 27, 28]

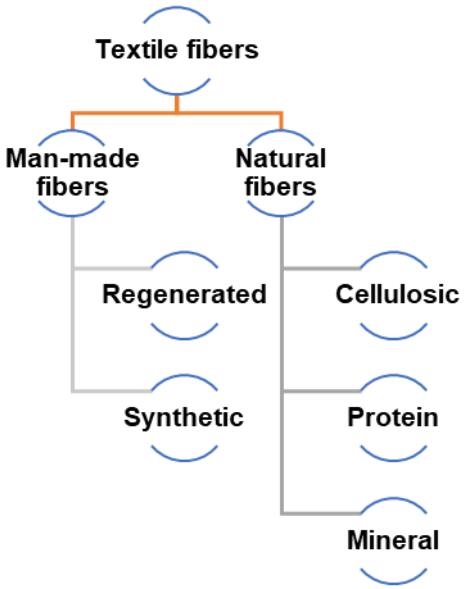

Figure 2.1. Textile fiber classification.

The production of natural cotton fibers uses arable land and is also responsible for the consumption of considerable amounts of fresh water, fertilizers, and pesticides.[29] The expected future global population growth will further heighten the competition for land, energy, and water.[30] Consequently, alternatives to cotton, such as other cellulose based fibers one example being regenerated cellulose fibers that can use wood as a source material, will become more interesting.[27]

A yarn can be described as an assembly of staple fibers or filaments of continuous length that are either twisted or straight. Many natural fibers are staple fibers, with a length of 2-50 cm, and these are twisted to generate a continuous yarn. In contrast, synthetic fibers and silk consist of continuous filaments. A single filament is defined as a monofilament. Yarns with several filaments are referred to as multifilament yarns.[27, 31, 32]

Continuous man-made fibers can be produced through extrusion of a polymer solution or melt through a spinneret. The spinneret has one or a multitude of small openings and the size of

each opening determines the diameter of the spun filaments.[32] The solution spinning process is referred to as dry-spinning if the filament solidification is due to solvent evaporation. If the solidification, instead takes place in a coagulant bath, however, the process is called wet-spinning (Figure 2.2a). Dry-jet wet-spinning is a process, which combines both an evaporation and coagulation step (Figure 2.2b). For melt-spinning, a polymer melt is extruded through a spinneret and cooled before collection.[4, 32]

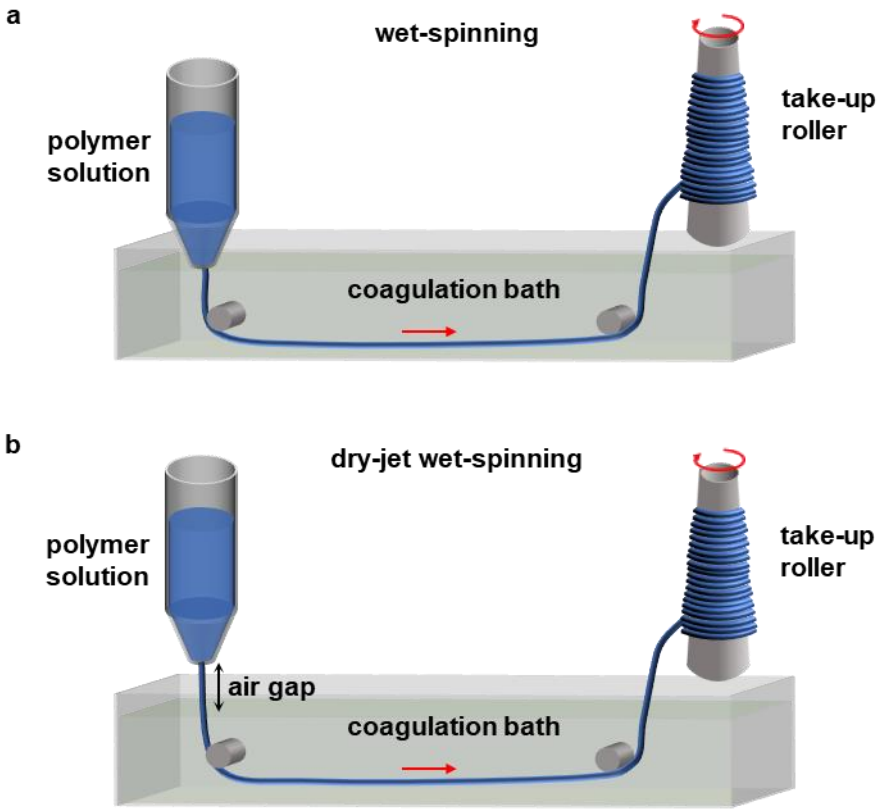

Figure 2.2. Schematic of the a) wet-spinning and b) dry-jet wet-spinning process.

The yarn numbering describes the fineness or coarseness of the yarn and can be defined in a direct or indirect way. For the direct system, the yarn number is the linear density of the yarn given in units of Tex, dtex or Denier. The linear density is the weight of the yarn per unit length,[31] i.e. grams per 1000 m yarn (= 1 Tex).[33]

Yarns can be assembled into fabrics through processes such as weaving and knitting (Figure 2.3).[32] Weaving can be accomplished with a loom or a weaving machine, and it is realized by interlacing warp and weft yarns. For knitting, interlocking loops between yarns instead create a textile fabric, which can be achieved by hand knitting and with knitting machines.[4, 34, 35]

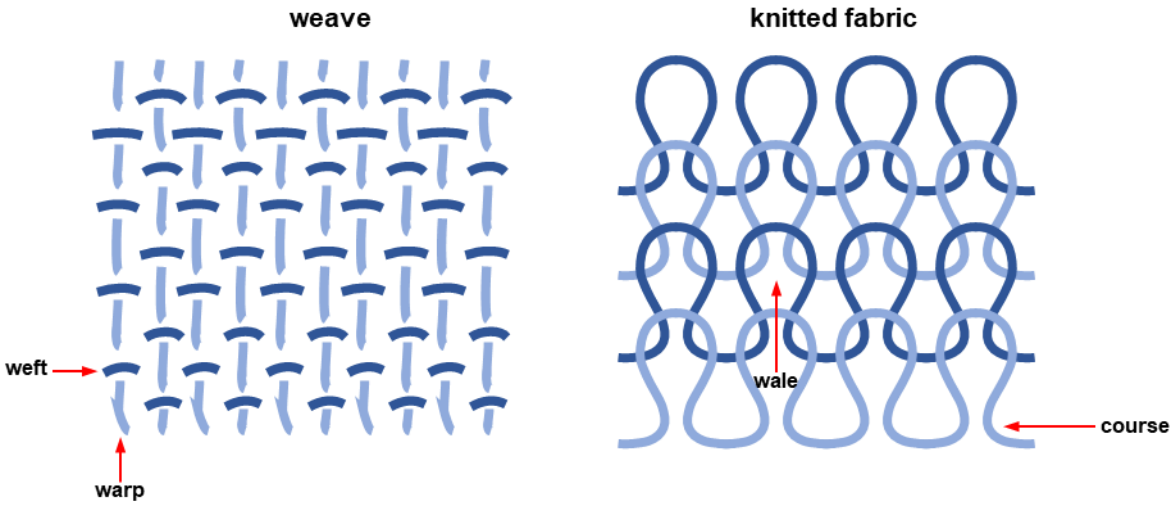

Figure 2.3. Schematic of a woven and a knitted fabric. Adapted with permission from ref [8]. Copyright 2021 Lund et al.

Textile fibers, filaments, yarns, and fabrics can undergo various treatments. For example, pre-treatments of textiles can be carried out to remove impurities and contaminants before further processing.[36] Dyeing and coating processes can be used to provide the textile fabric or fiber/yarn with added functionality or to just change the coloring of the material. Continuous or batch dye/coating processes can be utilized for dyeing/coating the substrate yarn or fabric, which can be achieved by passing it through a dye/coating bath (Figure 2.4). Further, the coating needs to show stability upon wash and wear if it is intended for wearable applications.[4]

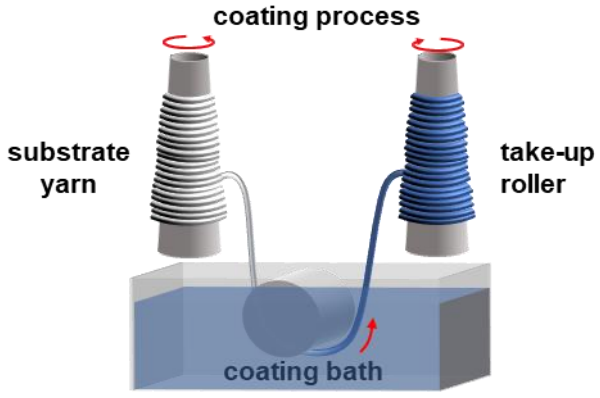

Figure 2.4. Schematic of a continuous textile yarn coating process.

3. Cellulose Materials

Cellulose is found in plants, such as trees and cotton, as one of the integral main components,[37] which provides stability to the plant cell wall.[38] Bacteria, algae, and fungi can also be sources for cellulose, thus making it the most abundant naturally occurring polymer.[37, 39] Cellulose is defined by its linear structure that is composed of D-glucopyranose repeating units joined by β-1,4-glycosidic bonds (see Figure 3.1 for the chemical structure). Further, every anhydroglucose unit rotates 180° regarding to its neighbouring unit. For every repeating unit of the cellulose chain there are three hydroxyl groups, one primary group and two secondary groups,[40, 41] that enable intra/intermolecular hydrogen bonds along and between the chains. The stiffness of the chain is due to intramolecular bonds, while intermolecular bonds give rise to a sheet structure arrangement.[41]

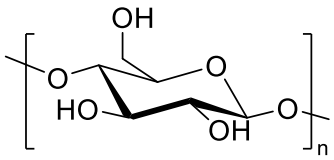

Figure 3.1. Chemical structure of the D-glucopyranose repeating unit.

Cellulose has several polymorphs that can be separated into Cellulose I, II, III and IV.[42, 43] The polymorph structure is influenced by the cellulose source, treatment, and extraction.[43] Native cellulose which is present in plants has the polymorph structure of Cellulose I. Further on, Cellulose II can be generated by either regeneration or mercerization of cellulose I.[37, 41] Cellulose II is observed to have a higher thermodynamic stability in comparison to Cellulose I,[44] while Cellulose I was shown to be stiffer.[44, 45]

Cellulose is hydrophilic and swells, yet it does not dissolve in water due to the highly ordered structure and hydrogen bonding network.[39, 41, 46] Cellulose is also insoluble in numerous organic solvents, yet there are systems that allow dissolution. By using indirect solvents, a cellulose derivative is generated which can be dissolved. This technique is utilized by the viscose process, where the cellulose derivatisation is accomplished with carbon disulfide (CS_2). The viscose process is industrially used to produce regenerated cellulosic fibers (Chapter 4). Direct cellulose dissolution can be achieved with *N*-methylmorpholine *N*-oxide (NMMO), which is also used for the fabrication of regenerated cellulosic fibers (Lyocell fibers). Hence, with direct solvents the cellulose dissolution can occur without derivatization.[41] Another class of direct solvents for cellulose dissolution are ionic liquids, which are salts with a melting temperature below 100 °C. A bulky organic cation and an inorganic or organic anion form the ionic liquid.[41, 47] The advantages with ionic liquids are its low vapor pressure, non-flammability as well as chemical and thermal stability.[48]

Cellulose is, as previously mentioned, one of the major components in wood. Trees are defined by their hierarchical structure (see Figure 3.2). Starting with the tree itself, which is

many meters tall, that is followed by the cross section in centimeters and growth rings that are on the millimeter scale. Further on, the cellular anatomy comprises features on the scale of tens of micrometers. The cellulose microfibrils, that are in a matrix of hemicellulose and lignin are on the order of tens of nanometers. Cellulose fibrils are composed of amorphous and crystalline regions.[49, 50]

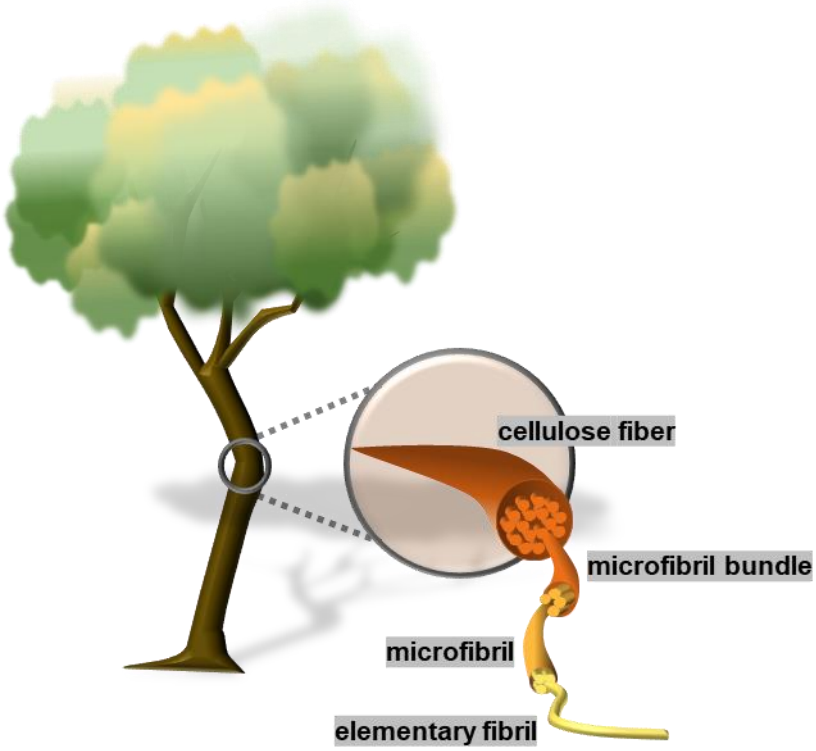

Figure 3.2. The hierarchical structure of wood. Adapted in part from ref [51] and ref [52].

When cellulose materials have one dimension in the nanometer range, it is referred to as nanocellulose. Due to different extraction sources for the nanocellulose materials, these will have different particle size, crystallinity, and aspect ratio. Nanocellulose materials have a number of attractive properties such as biocompatibility, thermal stability, high intrinsic stiffness and strength, as well as a high specific surface area. The mechanical properties make nanocellulose interesting reinforcing agents for nanocomposite materials.[53] Nanocellulose can be divided into cellulose nanocrystals (CNCs), bacterial nanocellulose (BNC) and cellulose nanofibrils (CNF).[49] The cellulose nanocrystals are short rod-like structures with high crystallinity. Instead, the longer cellulose nanofibrils are composed of considerable amorphous regions.[49, 53]

Mechanical disintegration of pulp is performed with a high-pressure homogenizer or sonication, if the pulp has been pre-treated, to produce CNFs. Chemical pre-treatments promote the disintegration, since charges on the fiber surface are generated, which result in electrostatic repulsion. Without a pre-treatment process, the energy requirement for the

mechanical disintegration process is high.[54] The carboxymethylation process is a pre-treatment procedure where the cellulosic surfaces become negatively charged upon introduction of carboxymethyl groups. The negatively charged surface will, as described previously, result in electrostatic repulsion, which eases the cellulosic fiber degradation into nanoparticles.[49] Another pre-treatment that aids the nanofiber isolation is 2,2,6,6-tetramethylpiperidine-1-oxyl (TEMPO) mediated oxidation, which introduces negative charges by converting the primary hydroxyl groups to carboxylates.[49, 54]

4. Cellulose-based Yarns and Textiles

Cellulose textile fibers can either be natural, like cotton fiber, or man-made like regenerated fibers.[27] The regenerated fibers possess attractive properties like comfortability and smoothness.[17, 55] The regenerated fibers present similar moisture management properties as cotton.[41] The main two types of regenerated cellulose textile fibers are Lyocell and viscose fibers. The fiber formation for these two processes can be divided into two steps, cellulose dissolution and regeneration via fiber spinning.[56]

The viscose process starts with dissolving wood pulp, by mixing the pulp with sodium hydroxide and forming alkali cellulose, which can react with carbon disulfide to generate sodium cellulose xanthate. To prepare the spinning solution, sodium cellulose xanthate is dissolved in weak sodium hydroxide solution. Continuous textile fibers are achieved by wet-spinning the spinning solution into a sulfuric acid bath. The volatile carbon disulfide and the by-products of the viscose process can result in environmental issues. Yet the viscose process is a prominent method for producing regenerated cellulose fibers.[57] Instead, Lyocell fibers are formed through direct dissolution of cellulose in *N*-methylmorpholine *N*-oxide (NMMO) and are presented as a more sustainable alternative to the viscose process. For this process, the wood pulp is mixed and dissolved in NMMO through heating. The spinning solution is spun into regenerated cellulose fibers using either a dry-jet or wet-spinning process.[41, 56, 58] As explained in chapter 2, filament solidification occurs for a wet-spun filament through coagulation in a coagulation bath, while dry-jet wet-spinning combines evaporation and coagulation for its solidification process. The dry-jet wet-spinning procedure includes an air-gap and a coagulation bath.[4, 32] The stretching that occurs in the air-gap can lead to alignment of the cellulose molecules within the as-spun filaments.[59] The NMMO is dissolved in the coagulation bath and the cellulose precipitates.[56] Stabilizers are necessary to reduce the possibility of runaway reactions, which can result from side reactions and by-product formation in the cellulose/NMMO/water system.[19, 41, 60, 61]

An alternative route for producing regenerated cellulose fibers is the Ioncell-F process that utilizes the ionic liquid 1,5-diazabicyclo[4.3.0]-non-5-enium acetate [DBNH][OAc] as the direct cellulose solvent.[19] Ioncell-F fibers are a specific type of Lyocell fibers.[41] Both dissolution and fiber spinning can be performed at a lower temperature compared to the NMMO-based Lyocell process, thus requiring less energy.[19, 61] Additionally, emissions from volatile organic compounds can be avoided when processing the cellulose with ionic liquids as the direct solvent, due to the low vapor pressure of ionic liquids.[59]

Ioncell-F fibers are produced through a dry-jet wet-spinning process.[41] The dry-jet wet-spinning process starts with extruding the spinning dope (polymer solution) through a multi-hole spinneret, which further passes through an air-gap where the fluid jet is stretched into a filament with the required diameter. Furthermore, the filament is immersed into the coagulation bath that consists of a non-solvent, which is water for the Ioncell-F process. The miscible solvent, which is the ionic liquid, leaches out of the polymeric filament and into the

coagulation bath where precipitation of the cellulose occurs.[19, 62] The coagulated continuous filaments can later be washed, dried, and gathered.[41]

Yarns are generated by assembling filaments or staple fibers, through mechanical twisting. Staple fibers possess a limited length while filaments are continuous. To make yarns from staple fibers, the process consists of carding fibers to make a web, followed by twisting the web into a sliver, which is an assembly of loose parallel fibers, finally the sliver is drawn and twisted to produce a yarn.[4, 31, 63, 64] Continuous Ioncell-F multifilaments have been utilized in this thesis as a substrate yarn for the manufacturing of electrically conducting yarns.

5. E-textiles

E-textiles are textiles with electronic functionality. Through the integration of diverse materials such as conductors, semiconductors and electrochemically active components, these e-textiles can be used to construct a myriad of wearable devices.[8]

5.1. Application Area

As introduced in Chapter 1, one of the intended application areas for e-textiles is health monitoring. The functionalization of textile materials into e-textiles allows the interface between textiles and skin to be accessed for sensing technologies, which can provide the users with information about their health.[65] The creation of e-textile sensing devices can for example enable long-term electrocardiography. Takamatsu et al. generated a method for patterning knitted textiles with conducting polymers. The process was utilized for the production of PEDOT:PSS electrodes that were coated with an ionic liquid gel, which facilitated recording of electrocardiograms.[1]

Furthermore, a power supply is required for the e-textile devices to function. For wearable applications it is favorable to exploit in-situ energy harvesting textiles that exploit surrounding sources of energy and are maintenance-free.[66, 67] Energy harvesting textile devices can be realized by exploiting the piezoelectric,[68] photovoltaic,[69, 70] thermoelectric[67] or triboelectric effect.[71] Specifically, the appeal with thermoelectric e-textiles is that these utilize the temperature gradient that already exists between the device wearer (surface body temperature) and the surroundings.[66]

5.2. Manufacturing Methods

E-textiles can be fabricated through a top-down approach, which constitutes printing, coating or the in-situ growth of a conducting material onto a substrate fabric.[72] Alternatively, a bottom-up approach can be employed that involves coating a substrate fiber/yarn with the conducting material or by using the conducting material for fiber spinning.[72] For the processes where a substrate textile fiber, yarn or fabric is used these materials will account for the structural integrity.[4] E-textiles for thermoelectric applications can be produced through both bottom-up and top-down textile processes. For example, Kirihara et al. produced a thermoelectric generator by using impregnated nonwoven fabric sections as one of the components to construct the device.[73] In contrast, Ryan et al. produced conducting yarns that were stitched into a fabric to create the energy harvesting device.[67] Moreover, the ambition for the e-textile manufacturing processes should be to enable mass production thus the processes should be scalable and produce resilient materials.[9]

5.3. Materials for E-textile Manufacturing

5.3.1 Conducting Materials

Metals are conducting materials that have a high conductivity (~ 10^5 S cm^{-1}) and are consequently employed as electrodes and interconnects. Metals that present a low toxicity, like gold, are interesting to use for wearable applications where the e-textile could be in close contact with the user.[8] Silver is often used due to its high conductivity and cost effectiveness, in comparison to gold.[72, 74]

Metal wire threads are commercially available, yet these can be stiffer and heavier in comparison to the ordinary textile fibers, which can culminate in complications for textile processing methods and affect the wearability. However, coating a substrate textile with for example silver metal nanowires or silver flakes creates a mesh, which reduces the amount of metal used as opposed to a solid metal thread. The reduced amount of metal will lower material cost and weight, while maintaining a high conductivity.[8, 74, 75]

Carbon allotropes, such as carbon nanotubes (CNTs) and graphene are often used as filler materials for creating polymer nanocomposites. CNTs display high stiffness in addition to high electrical (~ 10^4 S cm^{-1}) and thermal conductivities. The use of carbon nanotubes for wearable applications is of concern due to health risks associated with the materials.[76]

5.3.2 Semiconductors

Conjugated polymers are polymers that show conductive or semiconductive behaviour. As a conducting material, these conjugated polymers are interesting because these are lightweight, easy to process with adjustable conductivities.[77] The conjugated polymer backbone is comprised of alternating single and double bonds. In turn, the alternating double bonds give rise to delocalized π-electrons along the polymer backbone. Orbital interaction results in energy level splitting of the π- and π*-orbitals, with the former giving the valence band that is limited by the highest occupied molecular orbital (HOMO) (Figure 5.1). The π*-orbitals generate the conduction band that is initiated with the lowest unoccupied molecular orbital (LUMO). Further, the bandgap E_g is defined as the energy difference between LUMO and HOMO.[13, 78]

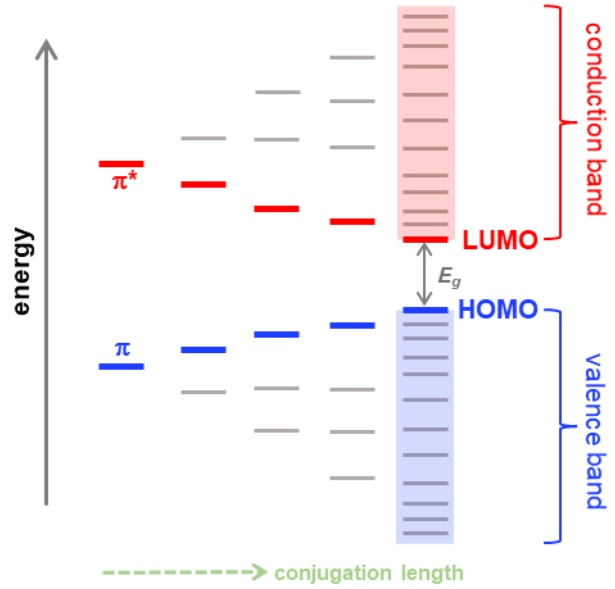

Figure 5.1. Energy level splitting of the π- and π*-orbitals with increasing conjugation length. Adapted with permission from ref [13]. Copyright 2016 The Royal Society of Chemistry.

Doping is performed to increase the electrical conductivity of the semiconductor (Figure 5.2). Doping is achieved either through an acid-base reaction or a redox reaction that constitutes a transfer of either an H^+/H^- (acid-base reaction) or an electron (redox reaction) between the polymer and the dopant.[13] Doping of the semiconductor generates radical anions or cations i.e. positive or negative polarons that can combine at high doping levels to produce bipolarons or polaron pairs. These polarons and bipolarons serve as charge carriers.[79]

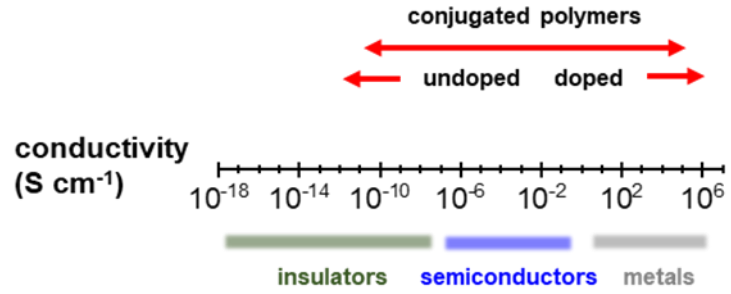

Figure 5.2. The conductivity of insulators, semiconductors and metals. Adapted with permission from ref [80]. Copyright 2015 The Royal Society of Chemistry.

PEDOT:PSS, which has been extensively studied for flexible electronics, is prepared through oxidative polymerization of EDOT in the presence of the oxidant $Na_2S_2O_8$ and polyanion PSS. PSS is charge compensating and further makes PEDOT:PSS water processable.[22, 81] The polymer:polyelectrolyte complex is commercially available as an aqueous dispersion.[26] PEDOT:PSS is described to have a core-shell structure in the aqueous dispersion with a PEDOT-rich core and PSS surrounding the core. Furthermore, high boiling additive such as

ethylene glycol (EG) and dimethyl sulfoxide (DMSO) have been reported to improve the conductivity of PEDOT:PSS by affecting the nanostructure.[13]

5.3.3. Electrochemically Active Materials

Polymers with mixed ionic and electronic transport can be employed as the active materials in organic electrochemical transistors (OECTs).[82] The hole conductivity of a (p-type) conducting polymer (Chapter 8), used in the OECT channel, can be altered with the injection of ions from an electrolyte while affected by an electric field.[82, 83] The doping level or redox state of the conducting polymer is modified.[83] Hence, OECTs have the capability of transducing ionic signals into electronic signals and can therefore be used for bioelectronics.[14]

5.3.4 Insulating Materials

Insulating materials are needed to produce e-textile devices where a substrate fiber, yarn or fabric is used together with a conducting material. For coated textile, the substrate will carry the mechanical load.[4] Moreover, insulating polymers can be used as matrices or binders to regulate the mechanical and rheological properties of conjugated polymers. The viscosity can be increased by including a small quantity of a high molecular-weight binder in a processing solution. Upon incorporation of increased quantities, the insulating polymer will function as the matrix and impart e.g., ductility or elasticity.[13]

6. Electrically Conducting Yarns

In this thesis, the bottom-up manufacturing approach of e-textiles is mainly considered since complex textile architectures with a wide range of devices can be generated by integrating several yarns with various functionalities into one fabric, for example through weaving or knitting.[8, 84] This concept was illustrated by Hamedi et al. through the production of wire-based electrochemical transistors with textile fibers, which can further be combined into logic circuits.[85] Further, Lee et al. produced conducting yarns for the manufacturing of knitted or woven thermoelectric textiles.[86]

6.1. Electrical and Electrochemical Properties of Interest for E-textiles

Electrically conducting yarns will need to show resistance towards abrasion, bending, and washing without losing electrical functionality. Common textile processing methods, like weaving and sewing, will expose the yarn to considerable abrasion. Hence, the durability of the yarn is of importance.[8]

Energy harvesting thermoelectric generators rely on the Seebeck effect, which is when a potential difference is produced upon subjecting a conducting material to a temperature difference (See Chapter 9).[87] The Seebeck coefficient α gives the magnitude of the Seebeck effect. Hole-transporting (p-type) materials have a positive coefficient while electron-transporting (n-type) materials have a negative Seebeck coefficient.[79] Both n- and p-type materials will be needed for the construction of thermoelectric generators. P-type conducting yarns can be realized using a number of materials including inorganic materials,[86] carbon nanotubes,[88, 89] graphene,[90, 91] and conducting polymers.[92] Reported n-type yarns have, however, been restricted to inorganic materials,[86] fullerenes,[92] carbon nanotubes,[89, 93] or graphene,[90, 91] since n-type conducting polymers do not offer sufficient air stability for use as e-textile materials. Yet the development of polymer-based textile generators is desired since conjugated polymers are based on abundant elements, often show a high degree of mechanical flexibility, and can be processed using cost-effective methods.[13]

Moreover, electrochemically active materials, such as conducting polymers, are needed for the fabrication of organic electrochemical transistor (OECT) channels. Electrically conducting fibers and yarns composed of conducting polymers can thus be used to construct textile OECTs.[85]

6.2. Manufacturing Methods

Electrically conducting yarns can be generated through fiber spinning or coating of a substrate yarns with conducting, semiconducting, or electrochemically active material (Figure 6.1).[8] When coating a substrate yarn, yarn with suitable properties can be selected with regards to

mechanical properties and processability.[94] The textile industry has a multitude of methods in place for processing of conventional yarns. Thus, these yarns could also be utilized for e-textile manufacturing.[84] For example, dyeing processes are already used within the textile industry. These methods can be used for both fabrics as well as yarns by immersing the textile material into a dyebath either through a batch or continuous process.[4]

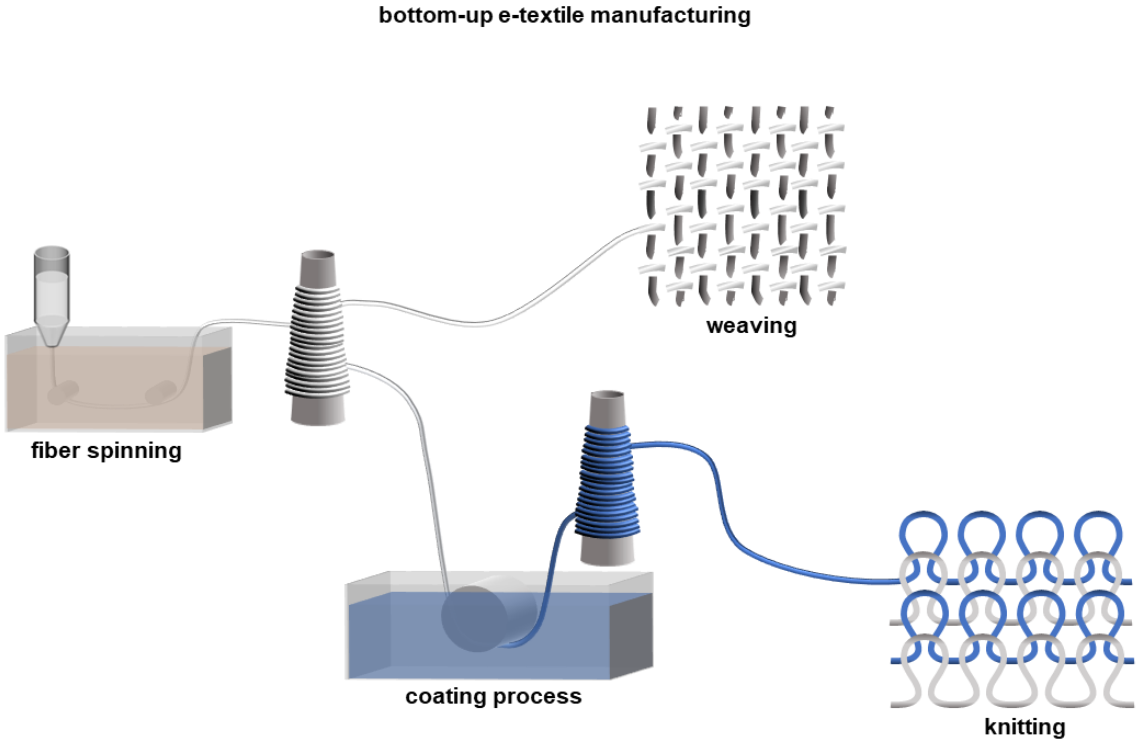

Figure 6.1. Schematic of manufacturing processes for fabricating e-textiles from electrically conducting fibers. Adapted with permission from ref [8]. Copyright 2021 Lund et al.

6.3 Literature Survey

A literature survey was carried out with the purpose of exploring the varying electrically conducting cellulose-based yarns and fibers that have been reported (Table 6.1 and Paper I). There was a lack of conducting cellulose yarns with a high electrical conductivity as well as a high degree of wash and wear resistance, which was also described in Paper I. Furthermore, another survey was conducted to investigate the fabrication of n-type yarns for textile thermoelectric generators (Table 6.1 and Paper IV). As previously stated, there was an absence of reported polymer-based conducting n-type yarns, which was assumed to be a consequence of insufficient air stability. There were, however, other examples of n-type materials used for textile thermoelectric applications such as the work of Pope et al. where cotton yarns were coated with fullerenes.[92]

Table 6.1. Overview of previously reported conducting fibers/yarns and the electrical conductivity (σ) of these materials.

	conducting component	manufacturing method	σ (S cm^{-1})	ref.
p-type	PEDOT:PSS	dip-coating, silk yarn	14	[25]
	PEDOT:PSS	R2R[a] dip-coating, silk yarn	70	[94]
	PEDOT:PSS + Ag nanowire[b]	dip-coating, silk yarn	320	Paper III
	PEDOT:PSS	dip-coating, cotton yarn	15	[25]
	PEDOT	oxidative chemical vapor deposition, viscose fiber	14	[95]
	MWCNT[c]	dry-jet wet-spinning, regenerated cellulose matrix	31	[96]
	p(g$_4$2T-T):CNF	dip-coating, regenerated cellulose yarn	3	Paper V
	PEDOT:PSS	R2R dip-coating, regenerated cellulose yarn	36	Paper I
	PEDOT:PSS + Ag nanowire	dip-coating, regenerated cellulose yarn	181	Paper I
n-type	Bi_2Te_3	electronspinning/sputtering/twisting, PAN[d]	8	[86]
	PCBM[e]	dip-coating, cotton	1×10^{-2}	[92]
	CNT[f]	direct spinning	7850	[97]
	graphene	self-assembly in tube mould	10	[91]
	BBL:PEI	spray-coating, regenerated cellulose yarn	8×10^{-3}	Paper IV

[a]R2R = roll-to-roll, [b]Ag nanowire = silver nanowire, [c]MWCNT = multi-walled carbon nanotubes, [d]PAN = polyacrylonitrile, [d]PCBM = [6,6]-phenyl-C_{61}-butyric acid methyl ester, [f]CNT = carbon nanotubes

High electrical conductivities can be achieved by fiber spinning conducting blends or composites. For example, wet-spun PEDOT:PSS fibers were generated by Sarabia-Riquelme et al. with a conductivity of up to about 3600 S cm^{-1} and a Young's modulus of 22 GPa, with a sulfuric acid drawing step. In addition, the conductivity could be further improved with the inclusion of a sulfuric acid immersion step.[21] Additionally, Rahatekar et al. produced a dry-jet wet-spun cellulose composite fiber by incorporating 10 wt% multiwalled carbon nanotubes, which resulted in a conductivity of 31 S cm^{-1}.[96] The health risks associated with carbon

nanotubes raises concerns for the employment of this material for wearable applications.

For the coating route, Ryan et al. produced PEDOT:PSS dyed silk and cotton yarns through batch processing. The developed yarns resulted in a bulk electrical conductivity of 14 and 15 S cm^{-1}, respectively. Furthermore, the PEDOT:PSS coated silk yarn could sustain bending and washing.[25] My master thesis resulted in further development of this process into a continuous roll-2-roll method.[94] A conducting silk yarn was obtained with a conductivity of 70 S cm^{-1} that could be processed with a weaving loom to produce a textile keyboard.[94] Further, conducting textiles can be produced by polymerization of conducting polymers onto yarns and fibers. This is exemplified by the work of Bashir et al. where oxidative chemical vapor deposition was used to coat viscose fibers with PEDOT. An electrical conductivity of 14 S cm^{-1} was obtained for the conducting textile.[95]

7. Preparation of Electrically Conducting Yarns

This chapter will introduce the different types of conducting yarns that were produced, the applications these yarns were intended for, and the manufacturing methods will be described as well. Mainly, the focus was to produce yarns with suitable electrical properties for thermoelectrics. For thermoelectric applications, there is a need for various building blocks when constructing such devices. Both n- and p-type materials are needed for the design of thermoelectric devices (See Chapter 9 for further details).

The electrically conducting yarns described in this thesis were generated mainly by coating a regenerated cellulose yarn with conducting polymers. Cellulose-based yarns are commonly used in the textile industry. Various dyeing processes are also used in the textile industry. The methods used for producing the conducting yarns could potentially be compatible with current textile manufacturing.

7.1. Roll-to-roll Coated Yarns

As stated in Chapter 6, Ryan et al. produced an electrically conducting silk yarn by using a batch process where the yarn was submerged in PEDOT:PSS dye bath.[25] The batch process illustrated the viability of the fabrication method for the creation of conducting silk yarns. However, a continuous coating process is preferable for further development since a larger quantity of yarn can be generated in a reproducible manner.

A roll-to-roll method was developed that consists of the substrate yarn being immersed in a coating bath, dried at 100 °C upon leaving the bath, and collected onto a take-up roller (Figure 7.1). The coating bath consisted of an aqueous PEDOT:PSS dispersion (1.1−1.3 wt % solid content) and a high boiling additive such as ethylene glycol (EG) which was utilized to increase the electrical conductivity of PEDOT:PSS. In addition, dimethyl sulfoxide (DMSO) was employed to increase the electrical conductivity of PEDOT:PSS through a post-treatment step where the coated yarn was immersed in DMSO. The passage of the yarn through the coating bath is motorized and consequently the residence time within the bath can be controlled, which results in a more homogeneous coating along the length of the yarn.

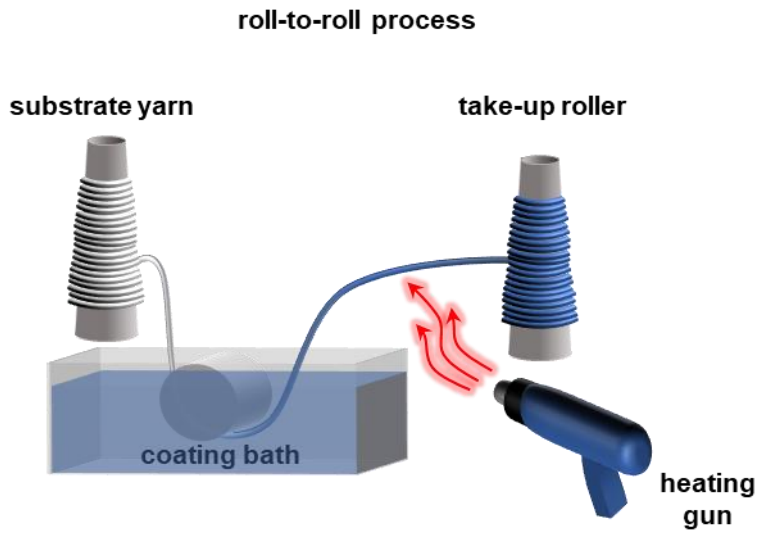

Figure 7.1. Schematic of the roll-to-roll coating process.

7.1.1. PEDOT:PSS dyed Silk Yarns

The roll-to-roll protocol was developed during my master thesis together with S. Hultmark to generate PEDOT:PSS coated silk yarns.[94] *Bombyx mori* silk yarns were used, which are produced as continuous filaments by the larvae of *Bombyx mori* silkworms.[98] The protein sericin covers the fibroin filaments and can be removed from the fibroin core with degumming procedures. The resulting material displays a high degree of biocompatibility and has been of interest for biomedical applications.[98, 99] Degummed silk yarns were pre-washed and dyed with PEDOT:PSS using the roll-to-roll process to produce a wash and wear-resistant conducting yarn. The yarn was woven to fabricate a textile keyboard that functioned via capacitive touch sensing. Further, an e-textile circuit was produced through machine embroidery with the assistance of C. Bunnfors and R. Carlsson at ACG Nyström.[94]

7.1.2. PEDOT:PSS Coated Cellulose Yarns

Conducting yarns were also produced by coating regenerated cellulose yarns with PEDOT:PSS (Paper I). Since cellulose is a widely occurring natural polymer[37, 39] it is advantageous to use this material for e-textile production. Furthermore, regenerated cellulose yarns produced via the Ioncell-F process can use a varied feedstock, even cellulosic waste products like paper and cardboard.[19, 20] In addition, the aqueous PEDOT:PSS dispersion is commercially available, which is an asset when producing large quantities of conducting yarns through a continuous coating process.

For the continuous process, the residence time of the yarn within the PEDOT:PSS + EG coating bath is controlled since the yarn passage is motorized, which provides an even coating layer along the length of the yarn. Yet the roll-to roll process is also restricting in the sense that each yarn segment will have a shorter time in the coating bath. The concentration of the

aqueous PEDOT:PSS dispersion can be increased through water evaporation. The coating layer of yarn becomes thicker when the yarn is coated with a dispersion that has a higher viscosity.[94] The transferred amount of the conducting material to filaments can also be increased by repeating the coating cycle.

The PEDOT:PSS cellulose yarns were used as the source-drain electrode for an OECT. The OECT devices were prepared and characterized together with I. Öberg Månsson (Chapter 8). Further, the p-type yarn was used to produce a textile thermoelectric generator (Chapter 9).

7.2. Dip-coated Yarns

7.2.1. PEDOT:PSS/Silver Nanowire Coated Cellulose and Silk Yarns

Substrate yarn, which was either regenerated cellulose or silk, was coated by a batch process with a composite coating of silver nanowires and PEDOT:PSS (see Paper I and III). Together with Prof. B. Hwang the cellulose yarn was dip-coated with a silver nanowire dispersion followed by drying at 80-90 °C for a couple of seconds (see Paper I and Figure 7.2). Dip-coating in the silver nanowire dispersion was repeated and followed by a final drying step at 180 °C. Subsequently, the yarn was dip-coated twice with a PEDOT:PSS dispersion, which also contained EG, and finally the yarn was dried at ~100 °C.

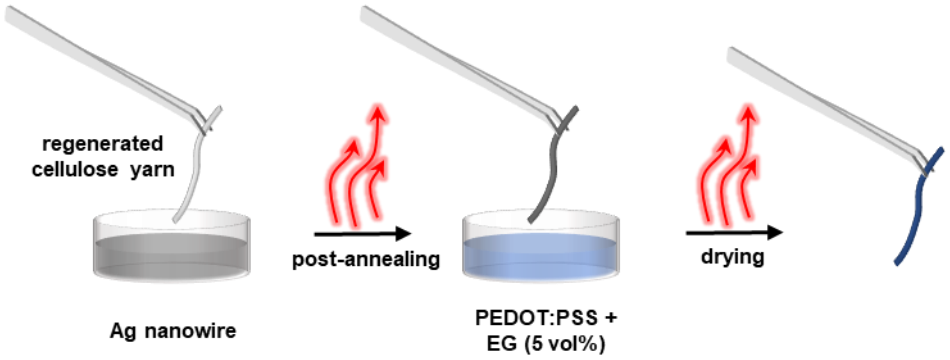

Figure 7.2. Schematic of the dip-coating method for producing PEDOT:PSS/Ag nanowire coated yarns.

This method of coating a substrate yarn with Ag nanowires and PEDOT:PSS was developed by Prof. B. Hwang and used to produce PEDOT:PSS/Ag nanowire coated silk yarns (Paper III). The degummed silk yarn was prewashed before coating the yarn with Ag nanowires. This was followed by immersing the yarn into a PEDOT:PSS + EG coating bath, which is the same coating bath that was developed for the roll-to-roll coating process. Furthermore, these conducting silk yarns were used by Hwang et al. to produce a thermoelectric device (See chapter 9) and a woven Joule heating element. By employing metal nanowires such as silver

nanowires for the yarn coating one obtains a yarn with a high conductivity, which can be used as a material for electrical connectors.

7.2.2. P($g_4$2T-T)/Cellulose Nanofibril (CNF) Coated Cellulose Yarns

Nanocomposites of a polythiophene with tetraethylene glycol side chains, p($g_4$2T-T), and cellulose nanofibrils (CNFs) were produced with the purpose of modulating the mechanical properties of the polymer without sacrificing its electrical properties (Paper V). Together with Dr. M. Mone, p($g_4$2T-T) was dissolved in dimethylformamide (DMF) and combined with carboxymethylated CNF dispersed in DMF. The mixture was stirred for 1 h at 35 °C. The nanocomposite was used to fabricate thin films (70 nm) by blade coating and thick films (100 µm) through drop-casting, as well as for the fabrication of conducting yarns. Tensile drawing revealed that the Young's modulus increased with the addition of CNF from 1 MPa for the neat p($g_4$2T-T) to 756 MPa for the nanocomposite containing 27 vol% CNF. The nanocomposites could also be doped with the p-type dopant 2,3,5,6-tetrafluoro-7,7,8,8-tetracyanoquinodimethane (F_4TCNQ). The average electrical conductivity of nanocomposites with a CNF content up to 20 vol% was 20 S cm^{-1}.

Further, a conducting yarn was produced by coating regenerated cellulose yarns with p($g_4$2T-T):CNF to illustrate the functionality of the material for e-textiles. The coating consisted of the nanocomposite with 9 vol% CNF and doping was done by coprocessing with 20 mol% F_4TCNQ. The coating was drop-casted with a micropipette onto yarns for several cycles with intermediate drying at 45 °C (Figure 7.3). The obtained p($g_4$2T-T):CNF coated cellulose yarn had a bulk conductivity of 3 S cm^{-1}.

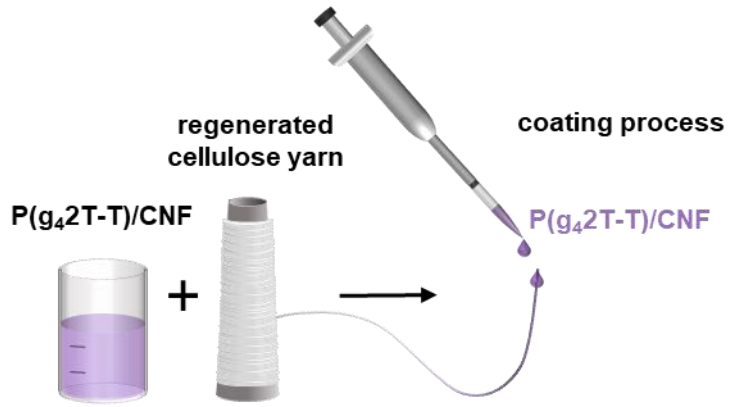

Figure 7.3. Illustration of the process of coating a cellulose yarn with p($g_4$2T-T):CNF.

7.3. Spray-coated Yarn (BBL:PEI Coated Cellulose Yarn)

Reported n-type (electron-transporting) yarns have been produced utilizing Bi_2Te_3,[86] fullerenes,[92] graphene[90, 91] or carbon nanotubes[89, 93] for yarn fabrication. Instead, n-type polymer-based yarns have not been reported, presumably because of limited air stability of n-

type conducting polymers. Polymer-based n-type yarns are an attractive avenue to explore due to the advantages of conjugated polymers, such as being lightweight and flexible.[13, 77] Furthermore, the health and environmental concerns linked to carbon nanomaterials also encourage the development of polymer-based n-type yarns.

For the manufacturing of n-type yarns, a poly(benzimidazobenzophenanthroline): poly(ethyleneimine), BBL:PEI, ink (Chapter 1) was chosen as the conducting material, which was used to coat regenerated cellulose yarns (Paper IV). The electrical conductivity of the ink was reported to be σ = 8 S cm^{-1} when BBL was processed together with PEI from ethanol.[26]

Preliminary studies were performed together with Dr. C. Yuan, to investigated whether a dip-coating or spray-coating process with ethanol-based BBL:PEI ink (1:1 weight ratio) would generate a more homogenous conducting layer on the yarn. The yarn was dip-coated by immersing the yarn four times into the ink or spray-coated by spraying the BBL:PEI ink onto ~1 cm long segments of the yarn at a time (see Paper IV for experimental details and Figure 7.4). A thermal treatment of the coated yarns in inert atmosphere (140 °C for 2 h under nitrogen) was required.[26] The reason for the thermal treatment is that the electron transfer from the amine-based PEI to the conjugated BBL polymer backbone is thermally activated. The positive charges on PEI balance the negatively charged polarons on BBL, yielding an n-doped all-polymer blend.

The quality of the coating layer was evaluated by measuring the electrical resistance of the conducting yarns. The dip-coated yarn featured segments with high resistance, which implied that the coating was not uniform. Instead, the spray-coated yarn was electrically conductive along the entire length and was thus selected for further investigation.

An insulating layer composed of the elastomer polystyrene-*b*-polyisoprene-*b*-polystyrene (SIS) was applied by pipetting droplets of SIS in toluene onto the conducting yarn (Figure 7.4) to improve the electrical stability at ambient conditions. We used the n-type yarn, together with the p-type PEDOT:PSS coated cellulose yarn, to construct a polymer-based textile thermoelectric generator.

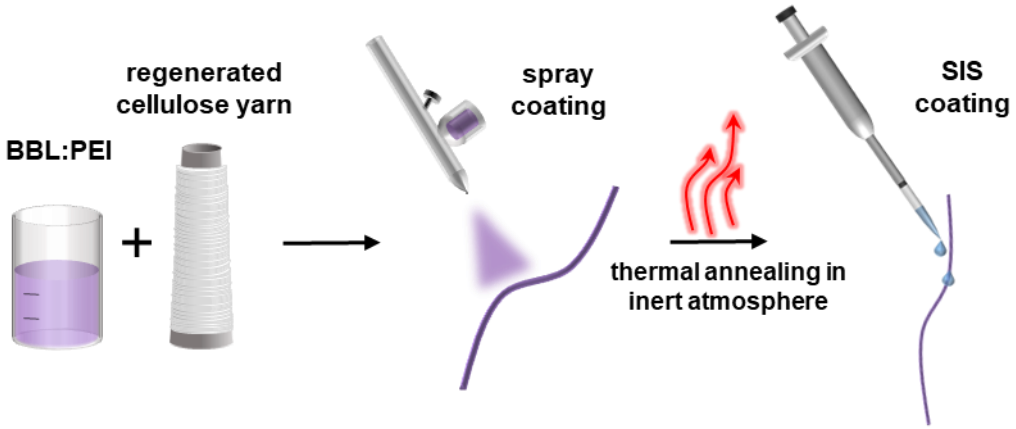

Figure 7.4. Schematic of the BBL:PEI spray-coating process.

7.4 Wet-spun fiber (PEDOT:PSS/CNF filaments)

Both PEDOT:PSS and CNF have been used previously to produce wet-spun fibers.[21, 100-102] For PEDOT:PSS, several non-solvents have been employed for the coagulation bath such as acetone, isopropanol and sulfuric acid.[21, 100, 101] For example, Dr. Y. Kim produced wet-spun PEDOT:PSS fibers by spinning the dope into a sulfuric acid coagulation bath.[103] The obtained fiber reached an electrical conductivity of 830 S cm^{-1}. Higher conductivity values can be reached for electrically conducting yarns if these are generated via fiber spinning of the conducting material, as opposed to yarns obtained through coating procedures where the main component is an insulating substrate yarn.

Wet-spinning of PEDOT:PSS filaments was also explored in this thesis, however, with the addition of CNF to the spinning dope. CNF was added to evaluate the impact on the fiber spinning process and on the filament itself. Carboxymethylated CNF, with a degree of substitution of 0.1 was used, which had been provided by Research Institutes of Sweden AB (RISE). A syringe pump (Harvard Apparatus Inc) was used to pump the spinning dope through a blunt needle into the coagulation bath. The spun fiber was collected onto a motorized take-up roller.

Initially, the spinning dope consisted of a ratio of 0.8% PEDOT:PSS, 1.0% CNF and 98.2% water. The spinning dope was spun via an 18-gauge blunt needle into an acetone coagulation bath (Figure 7.5a). The electrical conductivity of the filament, which given relative to the cross-sectional area of the filament, was obtained by measuring the resistance of a certain sample length (see Chapter 8). The conductivity was 4 S cm^{-1} for the PEDOT:PSS/CNF filament, by assuming a circular cross-sectional area. By following some parts of the PEDOT:PSS fiber spinning method described by Sarabia-Riquelme et al.,[21] the conductivity for the PEDOT:PSS/CNF filament. The pristine aqueous PEDOT:PSS dispersion was concentrated from a solid content of initially 1.3 to 2.5 wt% by evaporating water. Further, DMSO was added to the concentrated PEDOT:PSS dispersion. CNF was stirred into the spinning dope with an overhead stirrer for 2 h, sonicated for 30 min, and degassed in a vacuum oven at room temperature for a couple of minutes. For the spinning process (Figure 7.5b) a 27-gauge blunt needle was used with a 5 µl filter and a 1 ml syringe. The spinning dope consisted of a ratio of 2.35% PEDOT:PSS, 0.04% CNF, 4.69% DMSO and 92.9% water. The spinning dope was spun into an acetone coagulation bath. The obtained filament had a conductivity of ~ 125 S cm^{-1} (assuming a circular cross-section). The initial conductivity result of the produced filament was promising when compared to the recently reported the wet-spun PEDOT:PSS/CNF filament of Fall et al., where an electrical conductivity of 150 S cm^{-1} was obtained.[104] To obtain wet-spun PEDOT:PSS filaments that have a higher electrical conductivity the filaments can instead be spun, drawn or post-treated using concentrated sulfuric acid.[21, 100] However, this project came to a halt after initial trials with concentrated sulfuric acid due to the safety risks associated with it and in combination with working alone during the pandemic.

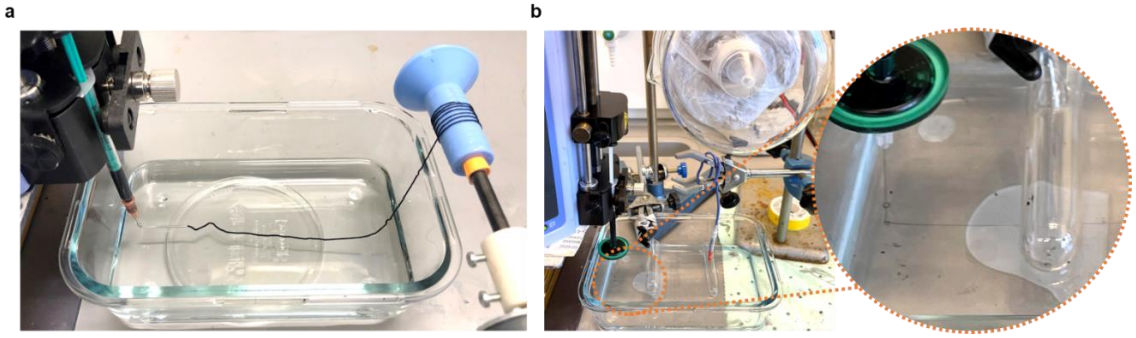

Figure 7.5. Wet-spinning process for the preparation of a) PEDOT:PSS/CNF fibers and b) PEDOT:PSS/DMSO/CNF fibers.

8. Conducting Yarn Characterization

The characterization of electrically conducting yarn properties of interest, such as wash- and wearability can be performed through different methods. Standards are available but these are generally for fabrics, which requires a large amount of material to be produced. For example, ASTM D4966-12(2016) gives a testing method for investigating the abrasion resistance of fabrics, while ISO 7854:1995 details methods for evaluating the resistance of coated fabrics to damage induced by repeated flexing.[105, 106] When working with single fibers and yarns it is necessary to develop strategies that could be used to characterize and evaluate the material.

8.1. Electrical Conductivity

The electrical conductivity σ can be expressed with the following equation (eq. 8.1):

$$\sigma = \sum q_i n_i \mu_i \qquad \text{(eq. 8.1)}$$

where n_i is the charge carrier concentration, μ_i is the carrier mobility, and the electric charge of a charge carrier i is q_i. The charge carrier mobility is influenced by the electronic structure, as well as the nano- and microstructure of the material. The charge carrier concentration depends on the number of intrinsic charge carriers as well as extrinsic ones that are induced through, e.g., doping.[13]

The electrical resistivity ρ (Ω cm) is the inverse of conductivity (S cm^{-1}),[107] thus:

$$\sigma = \frac{1}{\rho} = \frac{L}{A \times R} \qquad \text{(eq. 8.2)}$$

The resistivity is related to the electrical resistance R (Ω) of a material segment with a length L (cm) and a sample cross-sectional area A (cm^{-2}).[107, 108] Electrical resistance is a measure of opposition to the current flow through a material.[109]

In this thesis, the bulk volume conductivity (S cm^{-1}) was considered for the produced conducting yarns, as opposed to using the value obtained by estimating the thickness of the conducting layer (Figure 8.1). The coating is not limited to the perimeter of the yarn, conducting material can also be found on the individual filaments. For coating procedures such as the roll-to-roll coating process, where the passage of the yarn in the coating bath is controlled, a homogenous coating can be achieved. The coating will be less homogenous for manual yarn coating processes; thus, an outer coating layer thickness cannot be defined. The

total cross-sectional area of the yarn was used for calculating the bulk volume conductivity (eq. 8.2). For coated yarns, the volume will mostly be comprised of the insulating filaments and the voids between filaments. The conductivity is lower when considering the bulk rather than only the conducting component.

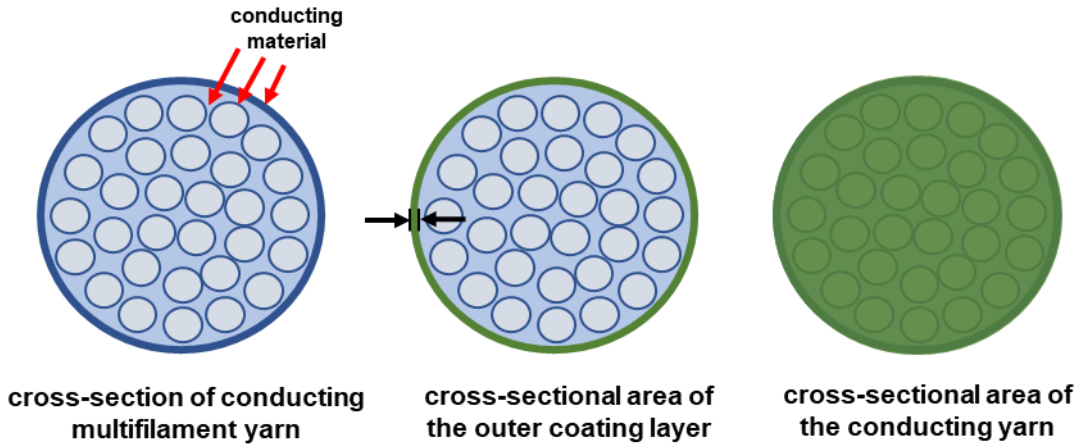

Figure 8.1. Schematic showing the cross-section of conducting multifilament yarn and the cross-sectional area (green) considered for conductivity calculations.

8.2. Electrical Characterization

8.2.1. 2-Point versus 4-Point Probe Configuration

To measure the electrical resistance between two points, a current can be applied to a sample that shows Ohmic behavior and the measured voltage can, with the help of Ohm's law ($R = V / I$) be employed to get the resistance. If a 2-point probe configuration is used, a contact resistance R_c can arise at the interface of the specimen and the probes, which adds to the total resistance that is measured.[110, 111] Specifically, the contact resistance is the resistance, which opposes the current flow across the interface between two materials in contact with each other.[112] The contact area between the two materials is limited as a consequence of surface roughness as well as the presence of possible insulating layers e.g. oxide layers on metals.[113] The contact resistance is influenced by the pressure applied to the contacts and whether the contacting surfaces are clean, smooth, or rough.[110]

A 4-point probe configuration will give a higher accuracy for resistance measurements in comparison to the 2-point configuration when the sample resistance is low. In case of the latter the contact resistance can significantly contribute to the total resistance. A linear 4-point measurement consists of four tips that are arranged linearly at equal distance for the characterization of bulk or thin film samples, as opposed to the Van der Pauw method, which places the 4-point probes at the boundary of a sample.[114, 115] Moreover, for the linear 4-point probe method a current is applied through the outer two probes while the voltage is measured across the two inner probes.[114] The contact resistance between the two inner probes and

specimen is avoided in the measured values with the employment of separate probes for current injection and voltage measurement.[116] Bashir et al. reported a set-up for resistance measurements of conducting yarns with a 4-point configuration. The set-up consisted of four brass wheels that were used as probes for the resistance measurement where the yarn could be fastened on one end and weighed down on the other end.[117]

The contact resistance can affect the e-textile device performance and it is therefore advantageous to minimize it. For electrical resistance measurements, silver paint was applied to get a better contact between the conducting yarn and the probes for the measurements that were performed via the 2-point probe configuration. Moreover, the value of the contact resistance was identified through a transmission line method[118] with the 2-point measurement, where the sample resistance of yarn segments with different lengths L can be compared and extrapolated to $L = 0$. Equation 8.3 for the electrical conductivity can be adjusted to include R_c thus the following expression is obtained:

$$\sigma = \frac{L}{A \times (R - R_c)} \qquad \text{(eq. 8.3)}$$

For conducting yarns with high resistance, the relative magnitude of the contact resistance can be smaller in comparison and will thus have a minor influence on the total value.

8.2.2. Electrical Stability

Long-term ambient stability of the electrical resistance was investigated by repeatedly measuring the yarn resistance over a period of time. The evaluation of the ambient stability demonstrates the duration for which a device such as a textile thermoelectric generator, where the internal device resistance influences power generation, can operate until loss of functionality. The gradual increase of electrical resistance was observed for PEDOT:PSS + EG coated yarns, which were post-treated with DMSO and stored in ambient conditions. After 460 days of storage, the resistance was measured to $R = 1.5 \times R_0$ for the PEDOT:PSS + EG coated cellulose yarn, which was produced by one roll-to-roll coating cycle (Figure 8.2).

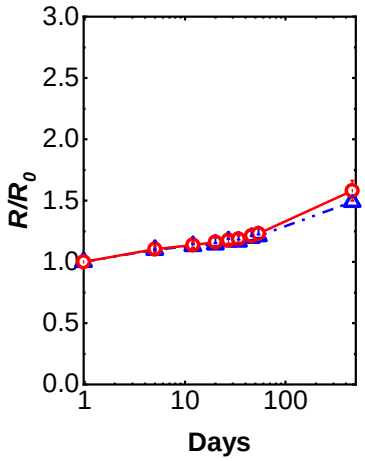

Figure 8.2. The ratio of electrical resistance R divided by the initial resistance R_0 of PEDOT:PSS + EG (DMSO post-treated) cellulose yarns coated through one (blue) or two (red) cycles, after storage under ambient conditions for 460 days. Reprinted with permission from ref [119]. Copyright 2020 American Chemical Society.

It has been claimed that PEDOT:PSS films have a gradual decrease in conductivity due to the hygroscopic nature of PSS, which leads to absorption of water from the atmosphere.[120-123] To improve the ambient stability of PEDOT:PSS films, Kim et al. proposed the removal of PSS through solvent post-treatment. Furthermore, the study showed that PEDOT:PSS + EG films, which had been post-treated in EG up to 30 min demonstrated a higher ambient stability, when compared to a film without post-treatment.[120]

Moreover, there is a lack of reported polymer-based n-type yarns, likely due to insufficient air stability of n-type conducting polymers. It was therefore of importance to show a promising level of air stability when developing a coated n-type yarn. Ryan et al. used the elastomer SIS as an outer protection layer for n-type carbon nanotube and poly(*N*-vinylpyrrolidone) coated PET yarns.[67] SIS was applied to the BBL:PEI coated cellulose yarns as an insulating barrier layer to investigate if the additional layer would improve the ambient electrical stability (Paper V). The electrical resistance of BBL:PEI coated yarns increased by about 10 to 60 times after 13 days of storage under ambient conditions (Figure 8.3). In comparison, the initial resistance of the n-type/SIS coated yarns only increased 5 times after 13 days at ambient conditions, indicating improved ambient electrical stability (Figure 8.3). The remaining change in electrical resistance was attributed to the unprotected yarn ends, which were not coated with SIS to facilitate points for electrical contact.

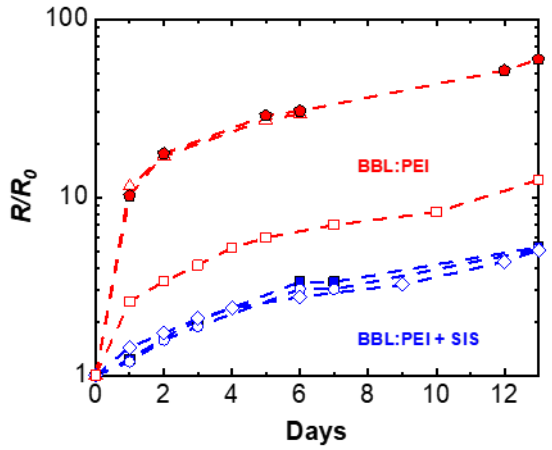

Figure 8.3. Electrical stability of BBL:PEI coated yarns stored at ambient conditions without (red) or with a SIS layer (blue) expressed as the ratio of electrical resistance R divided by the initial resistance R_0. The various symbols indicate different samples. R_0/L = 4.1, 8.8, 10.5 MΩ cm^{-1} for the SIS coated yarns, dried for 24 h at ambient conditions before electrical characterization; R_0/L = 1.7, 1.1, 4.2 MΩ cm^{-1} for as-prepared BBL:PEI yarns. Reprinted with permission from ref [124]. Copyright 2023 Advanced Electronic Materials published by Wiley-VCH GmbH.

8.2.3. Yarn Based Organic Electrochemical Transistor

Yarn based organic electrochemical transistors (OECTs) were prepared and characterized to investigate the electrochemical functionality of the PEDOT:PSS + EG coated cellulose yarn together with I. Öberg Månsson (Paper I). For this application, the PEDOT:PSS + EG coated cellulose yarn was used as the active component and also functioned as the source and drain elecrode. The gate electrode was a commercial silver-coated yarn and both yarns were in contact with an electrolyte (Figure 8.4a).

The functionality of the PEDOT:PSS-based OECT depends on the reversible reduction and oxidation process of PEDOT:PSS.[85] PEDOT:PSS-based OECTs work in depletion mode since PEDOT:PSS is oxidized in the pristine state. The OECT is ON without an applied gate voltage V_g, the holes in PEDOT are compensated by sulfonate groups from PSS. The OECT turns OFF with the use of a positive V_g because PEDOT is reduced and cations are injected from the electrolyte and neutralize PSS.[83, 125]

To illustrate and evaluate the function of the OECT, the output, transfer and transient characteristics can be investigated.[126] For the output characteristics, the source-drain current I_{sd} response was measured while the source-drain voltage V_{sd} was swept (Figure 8.4b). V_g was held during each sweep and then increased in steps for each sweep. Thus, I_{sd} was electrochemically modulated by applying different V_g at the gate electrode. Further, the

transfer characteristics were recorded by sweeping the gate voltage and recording the source-drain current as the source-drain voltage was held (Figure 8.4b). The transfer characteristics gives an ON/OFF ratio. The transient characteristics were recorded by measuring the source-drain current at a fixed source-drain potential while the gate voltage was switched between 0 V (ON) and a voltage which turns the OECT off. A switching speed can be obtained from the transient characteristics.[126]

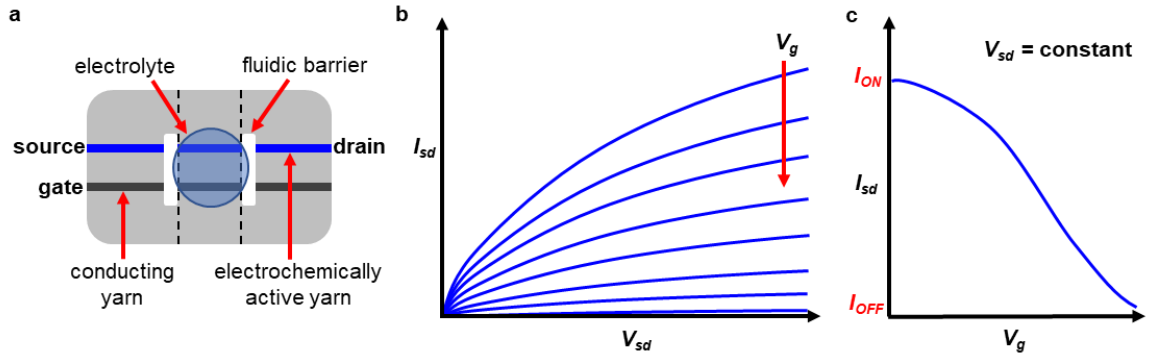

Figure 8.4. a) An example of a basic yarn based OECT. b) Output characteristics showing the source-drain current I_{sd} with the corresponding the source-drain voltage V_{sd} as the gate voltage is increased in steps. c) Transfer characteristics showing I_{sd} while V_g is swept and V_{sd} is held at a constant value. The source-drain channel is ON at $V_g = 0$ V and turns OFF with increasing V_g.

8.3. Mechanical Characterization

8.3.1. Tensile Testing

Tensile testing is often performed with textile fibers and yarns to investigate the mechanical properties of the materials. Stress can progressively be applied to the fiber/yarn, which leads to elongation that can be measured giving a stress-strain curve.[27] Stress is defined as the force per unit area, initial cross-sectional area for engineering stress and instantaneous cross-sectional area for true stress, while strain is the extension per unit length.[127-129] Fibers of varying sources generate distinct stress-strain curves, which is due to the structure of the material.[27]

One of the properties obtained from tensile testing is the Young's modulus, which corresponds to the slope of the stress-strain curve at the origin and gives an assessment for the stiffness of the fiber (Figure 8.5).[27] Furthermore, the yield point is reached when a further increase in stress makes the fiber lose the ability to recover its original shape.[130] At a certain point the fiber will rupture and the strain at break is the strain the yarn has experienced when it breaks. The fiber tenacity corresponds to the applied stress when the fiber breaks.

Moreover, toughness is determined from the total energy input until the fiber breaking point, which is the area under the stress-strain curve.[27]

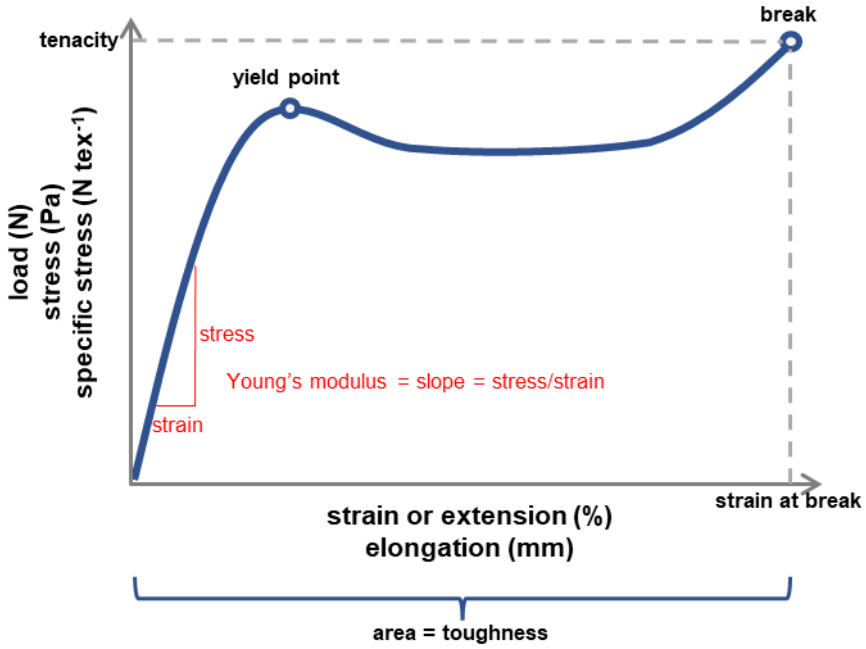

Figure 8.5. A general stress-strain curve for a semi-crystalline polymer at $T_g < T < T_m$. Adapted with permission from ref [4]. Copyright 2018 Elsevier B.V. All rights reserved.

8.3.2 Cyclic Bending

Bending tests were carried out to investigate the electrical resilience of the conducting yarns towards repeated deformation. Further, the bending test could give an indication of whether the conducting yarns are practical for device manufacturing and for use in wearables. The conducting yarns were subjected to repeated bending with a custom-built LEGO device built by Dr. A. Lund, with a bending curvature of a ~ 4.3 mm radius for the yarns, which were placed on a paper substrate (Figure 8.6a). The electrical resistance was measured every 100th cycle for a total of 1000 bending cycles using a 2-point configuration. There was only a slight increase in R/R_0, R_0 is the measured resistance prior to bending, for the once-coated yarn and no increase for the twice coated yarn after 1000 bending cycles (Figure 8.6b). This indicated that the twice coated PEDOT:PSS + EG coated yarns were highly resilient. Consequently, the yarns could be machine-sewn into a textile fabric for thermoelectric device fabrication. Further, the electrical resistance of the n-type BBL:PEI coated yarn increased by about 20% irrespective of the presence of the additional SIS coating (Figure 8.6c). The n-type yarn had a promising degree of robustness, which facilitated simple textile manufacturing methods, such as stitching.

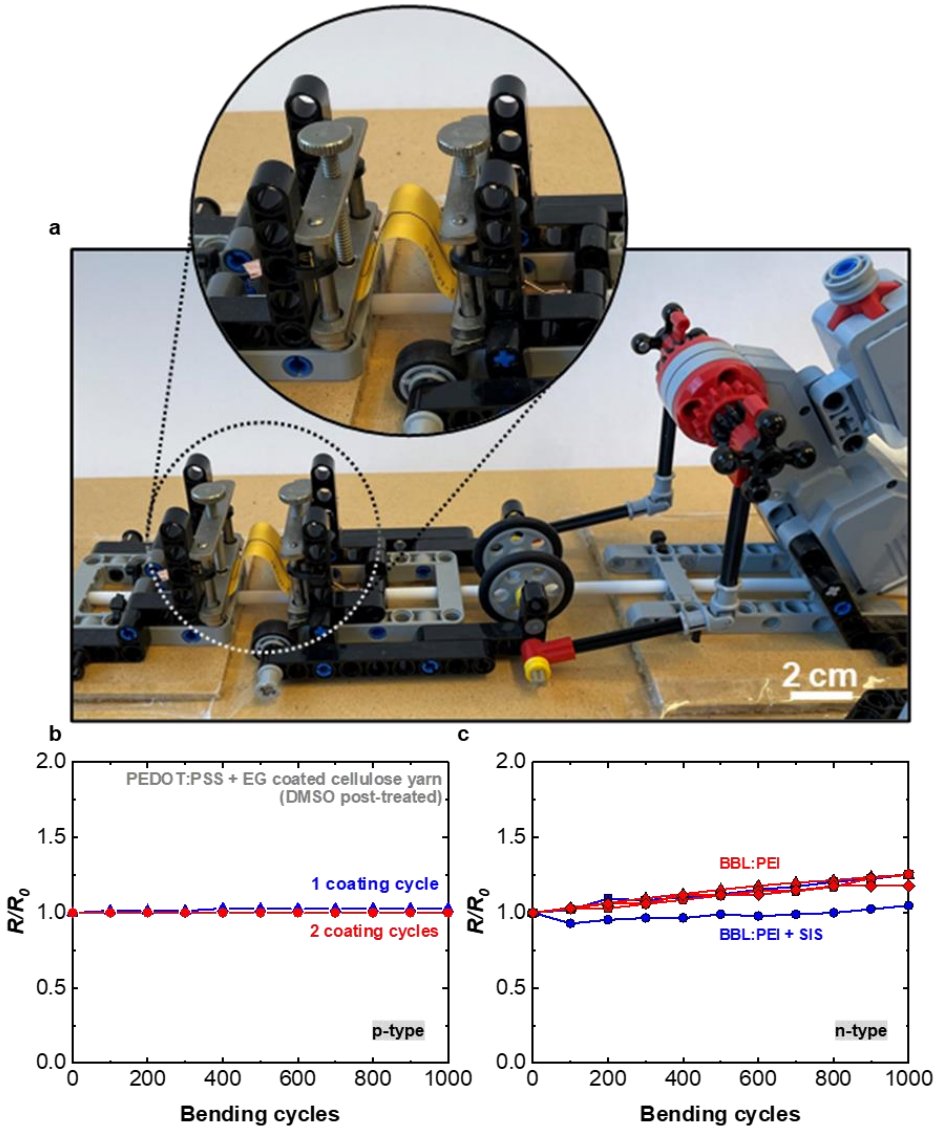

Figure 8.6. Photograph of the custom-built LEGO device used for bending tests with a mounted yarn. Electrical resistance R divided by the initial resistance R_0 measured after every 100 cycles during a total of 1000 bending cycles for b) PEDOT:PSS + EG (DMSO post-treated) cellulose yarns coated through either one (blue) or two (red) coating cycles and c) BBL:PEI coated yarn (red) and BBL:PEI/SIS coated yarn (blue). The various symbols indicate different samples. Adapted with permission from ref [119] and ref [124]. Copyright 2020 American Chemical Society. Copyright 2023 Advanced Electronic Materials published by Wiley-VCH GmbH.

8.3.3 Washing Test

For everyday use of e-textiles, it is important to evaluate the washability of the produced electrically conducting yarns. ASTM WK61480 is a proposed standard that is under development, and it is a test method that investigates the durability of smart garment textile

electrodes when exposed to washing and drying.[131] Further, there are standards like ISO 6330:2021 that give testing procedures for domestic washing and drying of textiles fabrics, garments and other textiles.[132] The sample property that was of interest for this thesis was the electrical resistance of coated yarns upon washing. Methods were developed for evaluating the washability of conducting yarns since there was no standard was available.

For PEDOT:PSS systems, since the polyelectrolyte PSS is water-soluble, washing could prove to be difficult. Massonnet et al. demonstrated that post-treatment with EG of PEDOT:PSS films enhanced the electrical properties and in addition increased the hydrophobicity of the film, which improved the stability towards water in comparison to a pristine PEDOT:PSS film. It was speculated that the improvement was due to partial removal of PSS from the film.[133] The regenerated cellulose yarn coated with a pristine PEDOT:PSS dispersion lost its coating in a matter of minutes when submerged into water (Figure 8.7a, left), whereas the yarn coated with the PEDOT:PSS + EG ink showed an improved stability in water (Figure 8.7a, right). Thus, EG was used together with PEDOT:PSS when fabricating the PEDOT:PSS-based conducting yarns (Paper I and III). To investigate the washability of the PEDOT:PSS + EG coated cellulose yarns, the yarns were stitched onto swatches and washed by Dr. A. Lund up to 10 times in a household washing machine using detergent (See Paper I for details). The resistance did not markedly change during the first five washing cycles for the twice-coated PEDOT:PSS + EG yarn, while the once coated yarn was able to withstand only three washing cycles (Figure 8.7b).

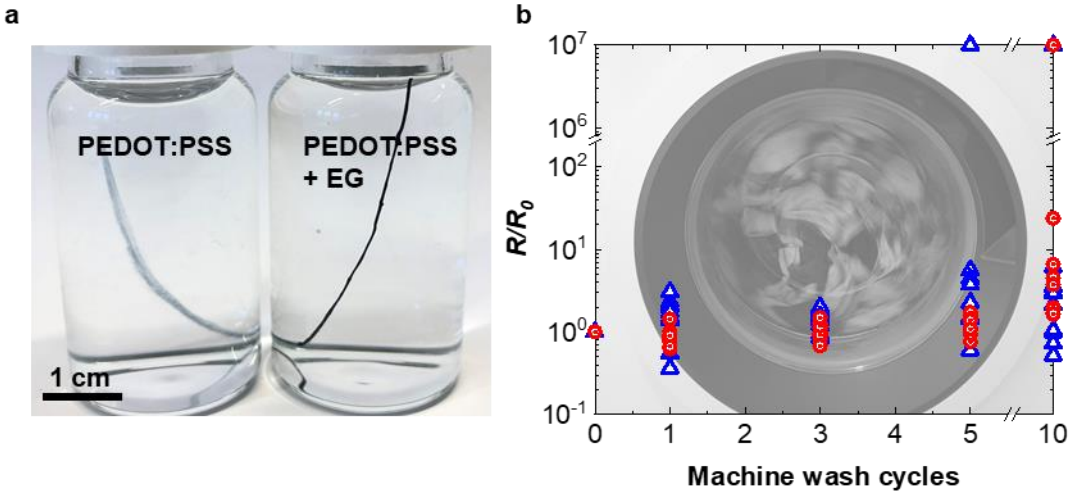

Figure 8.7. a) Photograph of pieces of cellulose yarn coated with PEDOT:PSS and PEDOT:PSS + EG, respectively, submerged in water for several minutes. b) R/R_0 of cellulose yarns with one (blue) or two (red) coating layers after up to 10 machine wash cycles. The outlier datapoints with a value of 10^7 correspond to segments whose resistance was too high to be measured. Reprinted with permission from ref [119]. Copyright 2020 American Chemical Society.

Furthermore, a trial was performed to compare the wash resilience between PEDOT:PSS + EG coated cellulose yarns and PEDOT:PSS + EG coated cellulose/chitosan yarn. Both the regenerated cellulose yarn and the composite yarn of cellulose/chitosan were produced by Zahra et al. using the Ioncell process.[134] The yarns were dip-coated once into a non-

concentrated PEDOT:PSS dispersion with added EG, to get a thin coating on the yarn, which could easily be removed upon bath sonication for the assessment of the coating resilience. The molecular structure of chitosan resembles cellulose apart from an amino group in the D-glucopyranose repeating unit.[134] The isoelectric point for chitosan is found around pH 9 and in acidic conditions it has a net positive charge due to the protonated amino group.[135] Ryan et al. argued that degummed silk, which similarly displays a net positive charge in acidic conditions, readily binds to PEDOT:PSS at the inherent low pH of the dispersion (pH 2) because of the negatively charged PSS.[25] For this purpose, it was of interest to evaluate if a substate containing chitosan that has been coated with PEDOT:PSS displays an improved washability (Figure 8.8).

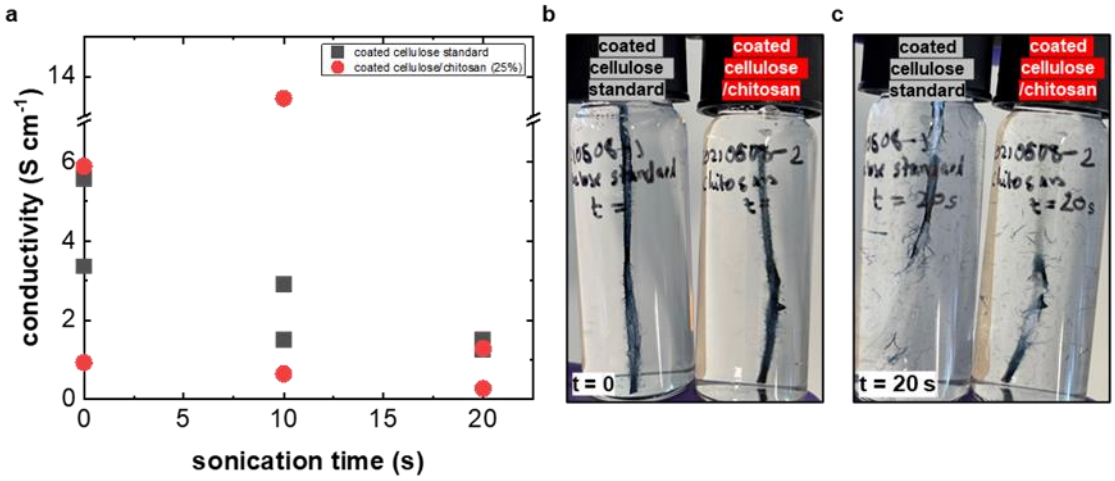

Figure 8.8. a) The conductivity of PEODT:PSS + EG coated regenerated cellulose (grey squares) and cellulose/chitosan (red circles) yarns after a sonication time 0 - 20 s. The coated yarns immersed in a vial with water b) before sonication and c) after 20 s of sonication.

The developed method to compare washability showed no significant change in the wash resilience for the PEDOT:PSS + EG coated yarn upon a change of the substrate yarn from cellulose yarn to cellulose/chitosan yarn (Figure 8.8). For future studies, it would be of interest to continue the exploration of washability by trying other coating and yarn combinations.

Moreover, for a summary of the produced conducting yarns mentioned in this chapter see Table 8.1, which includes some of the properties of interest for the development of e-textile devices that have been considered in this thesis.

Table 8.1. Overview of the some of the properties of the produced electrically conducting yarns.

Electrically conducting yarn	σ (S cm^{-1})	Electrochemically active	α (μV K^{-1})	Washability	ref.
PEDOT:PSS + EG coated cellulose yarn	36	Yes	14.6	+	Paper I
PEDOT:PSS + EG /Ag nanowire coated cellulose yarn	181	Yes	n.m.	n.m.	Paper I
PEDOT:PSS + EG coated silk yarn	74	Yes	15.0	++	[94]
PEDOT:PSS + EG /Ag nanowire coated silk yarn	320	Yes	0.8	++	Paper III
Wet-spun PEDOT:PSS:CNF + DMSO filament	125	Yes	n.m.	n.m.	-
p($g_4$2T-T):CNF coated cellulose yarn	3	Yes	n.m.	n.m.	Paper V
BBL:PEI coated cellulose yarn	8×10^{-3}	Yes	-79	n.m	Paper IV

n.m. = not measured, + = washable, ++ = very washable

9. Thermoelectric Textiles

Waste heat is often not exploited as an energy source despite it being a readily available resource. Upon exposure of a conducting material to a temperature gradient ΔT an electrical potential difference arises that can drive a current. This phenomenon is utilized by thermoelectric generators. Thermoelectric generators do not contain moving parts and can hence function long-term without maintenance.[13] For wearable applications, thermoelectric generators are interesting as a power source for e-textile devices, like sensors, where the temperature gradient between the wearer and the ambient surroundings could be utilized to operate the device.[79]

Commercial thermoelectric technologies are costly thus limiting extensive employment. To produce these devices, inorganics are utilized such as metal alloys that typically contain toxic elements, such as lead and tellurium. Furthermore, expensive microfabrication techniques are employed.[13, 79] Thermoelectric plastics can be processed using more cost-effective procedures from solution or melt. Specifically, conjugated polymers, which can be used for thermoelectric applications, consist of abundant elements (carbon, sulfur, nitrogen, oxygen, and hydrogen).[13]

9.1. Thermoelectric Effect

The thermoelectric effect can be divided into the Seebeck effect, Peltier effect and Thomson effect. The Seebeck effect is explained as the voltage produced when a material is exposed to a temperature gradient at open circuit conditions. Charge carriers, either holes or electrons, diffuse from the hot side as a consequence of the conducting material being exposed to a temperature gradient and accumulate at the cold material section.[87] The diffusion of charge carriers and their subsequent accumulation is counterbalanced by an internal electric field, a potential difference ΔV is generated.[13]

9.2. Seebeck Coefficient and Characterization

The Seebeck coefficient α is defined as the potential difference ΔV that results per temperature difference ΔT between the hot and cold side of the material:

$$\alpha = -\frac{\Delta V}{\Delta T} \qquad \text{(eq. 9.1)}$$

For n-type semiconductors with electrons as majority charge carriers the Seebeck coefficient is $\alpha < 0$, while for p-type semiconductors where the majority charge carriers are holes the Seebeck coefficient is positive, $\alpha > 0$.[13] A relevant material for thermoelectric applications

should have a high electrical conductivity σ to reduce losses as a consequence of Joule heating and a low thermal conductivity κ to minimize thermal losses because of heat flow between the hot/cold reservoir. The dimensionless figure of merit ZT gives a value that can be used to assess the thermoelectric efficiency of a material:[13, 79, 136]

$$ZT = \frac{\alpha^2 \sigma}{\kappa} T \qquad \text{(eq. 9.2)}$$

where T is the absolute temperature. However, the power factor $\alpha^2 \sigma$ is commonly used in the place of ZT for comparison since measuring the thermal conductivity can be difficult.[13]

For this thesis, the Seebeck coefficient was characterized by two procedures, which were used for ~5 mm length individual yarns (Paper I - IV) or for longer sample lengths (Paper IV). For the individual yarns, the Seebeck coefficient was determined by using a SB1000 instrument together with a K200 temperature controller (MMR Technologies). A ~ 5 mm long piece of yarn is mounted onto a sample holder that also holds a reference constantan wire, that has the same length. The temperature of the sample holder is raised up to a chosen temperature of 300 K. The voltage across the conducting yarn as well as the exact temperature were measured, which in this case was set to 300 K, and the measurement was also performed for the constantan wire. Thereafter, the resistor on the stage was employed to heat one end of the stage by applying a current and the voltage measurement was repeated. The Seebeck coefficient for the reference $\alpha_{reference}$ was known. By also including the measured voltage differences for the sample ΔV_{sample} and the reference $\Delta V_{reference}$, the Seebeck coefficient for the sample α_{sample} could be determined with the following expression:[111]

$$\alpha_{sample} = \frac{\alpha_{reference}}{\left(\Delta V_{reference} / \Delta V_{sample}\right)} \qquad \text{(eq. 9.3)}$$

Alternatively, the Seebeck coefficient for a reference BBL:PEI film and BBL:PEI/SIS coated cellulose yarn were determined by exposing the samples to different temperature gradients and measuring the generated voltage (Paper IV). The motivation for the different measuring procedure was that the previous method only required a ~ 5 mm sample length, and it was difficult to coat such a small length with SIS while leaving the ends uncoated to facilitate points for electrical contact. Thus, the alternative procedure was utilized for characterization of yarns that were already integrated into a thermoelectric device.

9.3. Thermoelectric Generators

Generally, the produced voltage from a single thermoelectric leg will be inadequate to power electronic devices, which can at a minimum require 1 V.[111] It is therefore necessary to connect several thermoelectric legs, thermally in parallel and electrically in series. A thermocouple is

the primary unit of a thermoelectric generator (Figure 9.1), which can also be referred to as a thermopile. Each thermocouple consists of two legs with Seebeck coefficients of opposite sign so that the generated thermovoltages do not oppose each other. N- and p-type legs are thus generally used in alternation to construct the thermoelectric generators.

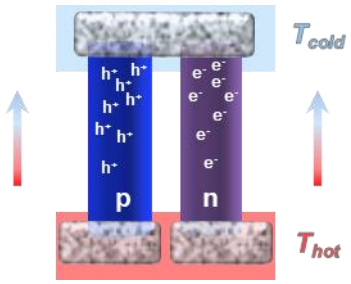

Figure 9.1. Schematic of a thermocouple consisting of a p- and n-type leg while exposed to a temperature gradient causing charge carriers to diffuse to the cold side.

Each individual leg adds to the total open-circuit voltage V_{oc} of a device, according to:[13]

$$V_{oc} = N(\alpha_1 - \alpha_2)\,\Delta T \qquad \text{(eq. 9.4)}$$

where N is the number of thermocouples, α_1 and α_2 are the Seebeck coefficients of the two types of thermoelectric legs.[13]

Due to the lack of reported polymer-based n-type yarns, alternatives were explored such as yarns containing conductors (i.e. silver) with a low Seebeck coefficient and used together with p-type polymer-based yarns for the fabrication of thermoelectric devices, thus $\alpha_1 > 0$ and $\alpha_2 > 0$ (Paper I - III).

For a thermoelectric generator, the maximum power P_{max} is realized if the external load and the internal resistance of the device are equal, $R_{load} = R_{int}$. The maximum power is then given by:[13]

$$P_{max} = \frac{{V_{oc}}^2}{4 \times R_{int}} \qquad \text{(eq. 9.5)}$$

9.4. Thermoelectric Textile Devices and Design

The design of textile thermoelectric devices can be divided into in- or out-of-plane devices. For wearable applications, out-of-plane devices are more practical since the temperature gradient between skin and the surroundings is along the thickness of the device.[137, 138] Additionally, for the design of an efficient thermoelectric device both n- and p-type materials are required. However, thermoelectric devices can be designed with p-type materials and low

Seebeck coefficient conductors as previously described.[79]

Conducting yarns can be utilized for thermoelectric device fabrication and these yarns allow for complex device architectures. For this thesis, electrically conducting yarns were manufactured and employed to produce thermoelectric devices. For Paper I-III the thermoelectric textile devices that were fabricated were out-of-plane (see Table 9.1). The creation of a polymer-based n-type yarn in Paper IV allowed for the fabrication of a textile thermoelectric device with both p-type and the n-type legs. Yet for Paper IV an in-plane device layout was selected due to the limited availability of the n-type yarns of a certain length.

Table 9.1. Overview of the reported textile thermoelectric generators from the papers included in this thesis with the maximum power P_{max} per 1 K and leg-pair.

device design	p-type material	n-type or low α conductor materials	number of thermocouples	P_{max} (nW per K and leg-pair)	paper
out-of-plane	PEDOT:PSS + EG (DMSO post-treated) coated cellulose yarn	commercial Ag-plated polyamide yarn	40	0.14	I
out-of-plane	PEDOT:PSS + EG (DMSO post-treated) coated silk yarn	commercial silverplated polyamide yarn	8	2.31	II
out-of-plane	PEDOT:PSS + EG (DMSO post-treated) coated silk yarn	PEDOT:PSS + EG/Ag nanowire coated silk yarns	1	0.32	III
in-plane	PEDOT:PSS + EG (DMSO post-treated) coated cellulose yarn	BBL:PEI/SIS coated cellulose yarn	4	3.5×10^{-5}	IV

Textile out-of-plane thermoelectric devices were fabricated in Paper II-III by Y. Tian via hand-embroidery through eight layers of felted wool fabric, which served as a thermal insulator. As embroidery became more difficult with a large number of fabric layers, the limit for the textile device thickness was 10 mm. Silver paint was applied between the thermoelectric leg-pairs to improve the electrical contact. PEDOT:PSS + EG coated silk yarn was used for the p-type leg in both Paper II and III while the other thermoelectric leg was composed of a commercial silver-plated yarn for Paper II. For Paper III, the interconnect was composed of a highly conductive and machine-washable PEDOT:PSS + EG /Ag nanowire coated silk yarn. The Seebeck coefficient of the PEDOT:PSS coated silk yarn had a positive value of 15.0 μV K^{-1}, and the PEDOT:PSS + EG /Ag nanowire coated silk yarns displayed a small positive value of 0.8 μV K^{-1}. The open circuit voltage $V_{oc}/\Delta T$ for the device, which consisted of only one thermocouple, was predicted to be $V_{oc}/\Delta T = (15 - 0.8)$ μV K^{-1} (eq. 9.4) (dashed line in Figure 9.2). The slightly lower measured generated voltage was attributed

to the presence of thermal contact resistances across the interfaces between the textile and the hot/cold side, respectively. Therefore, the thermocouple experienced a smaller ΔT compared to what the external temperature sensors measured which were attached to either side of the textile. A maximum power output $P_{max} = 22.3$ nW was measured at $\Delta T \approx 70$ K. The internal resistance of the thermocouple was ~10 Ω.

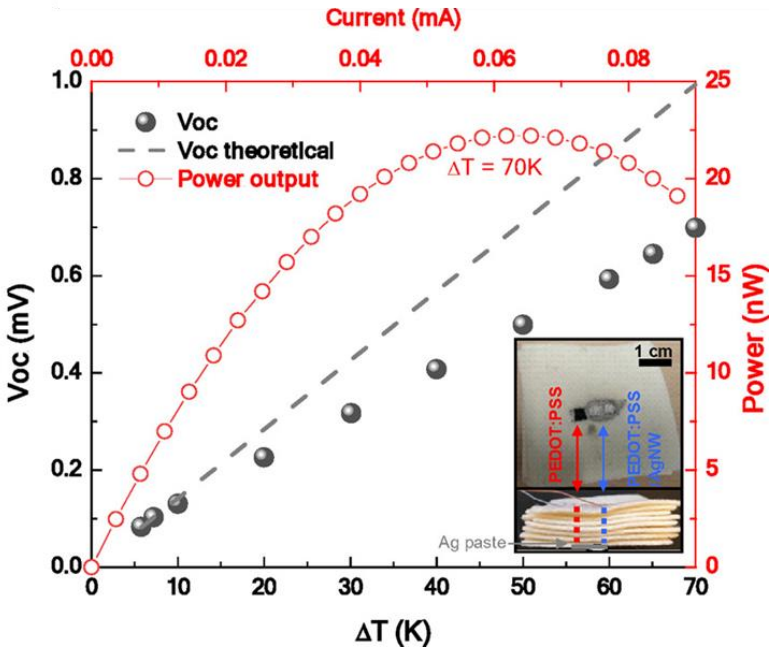

Figure 9.2. Open circuit voltage, V_{oc}, as a function of ΔT, and the power output, P, as a function of the measured current at ΔT = 70 K for a thermoelectric textile consisting of a single thermocouple. Insets are top and side view photographs of the out-of-plane thermoelectric device with one n-type leg composed of the PEDOT:PSS/Ag nanowire coated silk yarn and one p-type leg composed of the PEDOT:PSS + EG coated silk yarn. Reprinted with permission from ref [139]. Copyright 2020 American Chemical Society. [*thermoelectric textile device and data recording by Yuan Tian* (*Chalmers*)].

Moreover, the thermoelectric device fabricated in Paper II was composed of PEDOT:PSS + EG silk yarn and commercially available silver-plated yarn, with a Seebeck coefficient of $\alpha_1 = 14.3$ μV K^{-1} and $\alpha_2 = 0.3$ μV K^{-1}. The textile device had eight thermocouples and generated $P_{max} = 1.2$ μW at a temperature gradient of 65 K (2.3 nW per degree and leg-pair).

The voltage that is generated by a thermoelectric device is directly proportional to the number of thermocouples (eq. 9.4). Consequently, a textile manufacturing method that can be used to produce many textile thermocouples, while requiring a minimum of manual work, should be used. For the production of devices, machine sewing was explored, which allowed to shorten the fabrication time of each leg and simplified processing in Paper I.

A household sewing machine was used to sew an out-of-plane thermoelectric device into felted wool fabric (Figure 9.3a-d). The PEDOT:PSS coated cellulose yarn (Figure 9.3a) was

employed for the p-type leg (α_1= 14.6 μV K^{-1}) and the commercial silver-plated yarn (α_2 = 0.3 μV K^{-1}) for the second leg. The thread tension was adjusted, prior to sewing, to ensure that the conducting thread would completely penetrate the fabric so that it could be electrically connected on both sides of the fabric (Figure 9.3c). The two yarn types were separately stitched through three layers of felted wool fabric to form 40 out-of-plane thermocouples (Figure 9.3d). Silver paint was applied between the thermocouples and cured at 100 °C for 10 min.

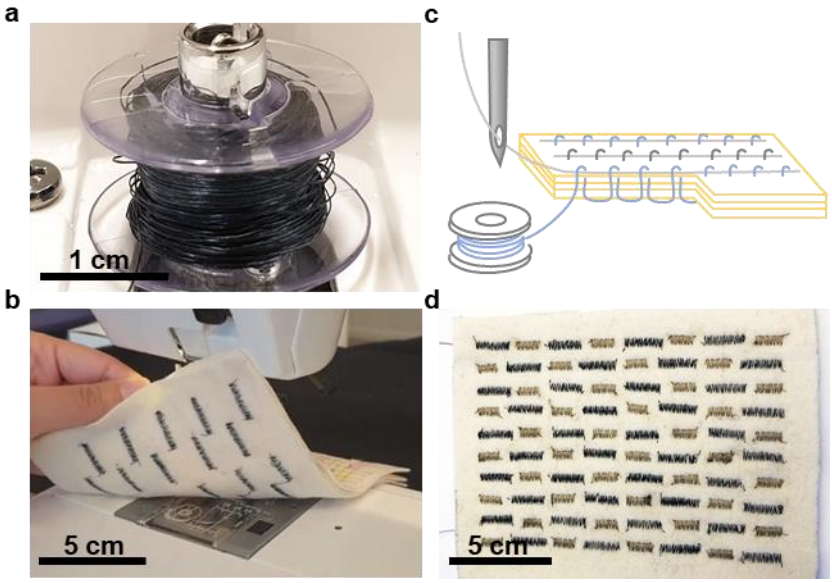

Figure 9.3. a) Conducting cellulose yarn wound onto a sewing machine bobbin. b) Machine sewing of an e-textile using the twice coated conducting cellulose yarn and a commercially available silver-plated embroidery yarn. c) Schematic of the machine sewn stiches. The conducting yarns (blue and grey lines) were wound onto bobbins, and the sewing machine settings were adjusted to ensure that the bobbin yarn was visible on both sides of the fabric after sewing so that it penetrates the full thickness of the multilayered fabric. d) A machine stitched all-textile thermoelectric generator with 40 out-of-plane thermocouples. Reprinted with permission from ref [119]. Copyright 2020 American Chemical Society.

The ideal open circuit voltage $V_{oc,max}$ was estimated to be 21 mV at $\Delta T = 37\ °C$ (eq. 9.4), while V_{oc} was measured to be 8.45 mV (Figure 9.4a). Thermal contact resistance limits the temperature gradient experienced by the thermopile ΔT_{tp} (Figure 9.4b,c) that can be described by:

$$\Delta T_{tp} = \Delta T \times \frac{K_{tp}}{K_c + K_{tp} + K_h} \qquad \text{(eq. 9.6)}$$

were the thermal resistance of the thermopile is given by K_{tp}. The contact resistance between the textile and cold reservoir is referred to as K_c and K_h is the contact resistance between the

textile and hot reservoir. Since $V_{oc}/V_{oc,max} = \Delta T_{tp}/\Delta T$, then:

$$V_{oc} = V_{oc,max} \times \frac{K_{tp}}{K_c + K_{tp} + K_h} \quad \text{(eq. 9.7)}$$

Subsequently, the ratio of thermal contact resistance of the thermopile to the total thermal resistance could be estimated to $K_{tp}/K_{tot} \approx 0.4$, signifying that ΔT_{tp} was reduced to less than half of the supplied temperature gradient ΔT. Further, a $P_{max} = 210$ nW was predicted (eq. 9.5), which closely matched the experimental value of 202 nW at $\Delta T = 37\,°C$ (Figure 9.4a).

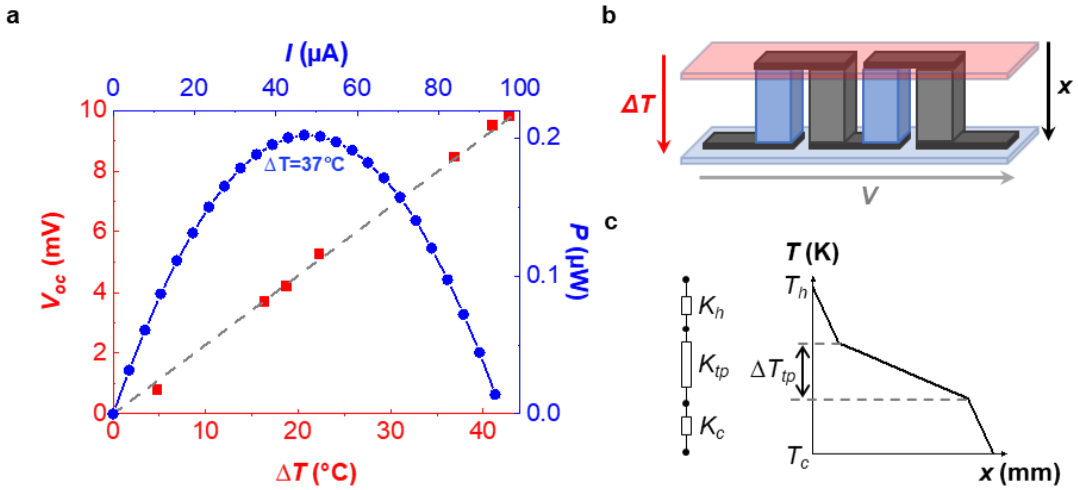

Figure 9.4. a) Open circuit voltage (V_{oc}) recorded at different temperature gradients ΔT (red squares), predicted $V_{oc,max} = 0.4 \times V$ (grey dashed line), and generated power P (blue filled circles+line) as a function of load current (I), for the all-textile thermoelectric generator. b) Schematic illustration of two thermocouples, the blue leg represents the conducting cellulose yarn and the grey leg is the commercially available silver-plated yarn, connected electrically in series and thermally in parallel. The light blue and light red volumes represent the thermal contact resistances on the hot and cold sides. c) Thermal circuit representing the thermopile: the thermal resistance of the thermopile (K_{tp}) is connected in series to the thermal contact resistances between the textile surfaces and the heat source (K_h) and the cold reservoir K_c), respectively. Reprinted with permission from ref [119]. Copyright 2020 American Chemical Society.

Given the ease of scalability of this processing technique, it is anticipated that fabrication of a textile that produces electrical power in the range of several microwatts is feasible. The number of thermocouples required for this machine-sewn thermoelectric device to generate 1 V, which is required for many types of devices, can be estimated with eq. 9.4 to 1890 thermocouples for a $\Delta T = 37$ K.

Furthermore, a prototype in-plane thermoelectric textile was produced in Paper IV by stitching yarns onto a felted wool fabric. The BBL:PEI/SIS cellulose yarn (α_2 = -272 μV K^{-1})

was used as the n-type leg and PEDOT:PSS coated cellulose yarn (α_1 = 14 µV K^{-1}) for the p-type leg (Figure 9.5a,b). The device consisted of four thermocouples where the n-type leg was composed of three yarns while the p-type leg was composed of two yarns. Silver paint was used as for the previous devices to improve the electrical contact between legs (Figure 9.5c). The internal resistance of the device was measured to be R_{in} = 180 MΩ. The open-circuit voltage V_{oc} increased linearly with the temperature difference with a slope of $V_{oc}/\Delta T$ = 1.0 mV °C^{-1} (Figure 9.5d). The predicted value of $V_{oc}/\Delta T$ = 1.1 mV °C^{-1} (eq. 9.4) was in good agreement with the measured value. Further, V_{oc} = 68 mV was measured for ΔT = 64 °C. The predicted power output was determined to be 6.4 pW and in reasonable agreement with the measured value P_{max} = 9 pW at ΔT = 64 °C. The difference in measured and predicted values may arise because of the variation in Seebeck coefficient of BBL:PEI coated yarns upon ageing.

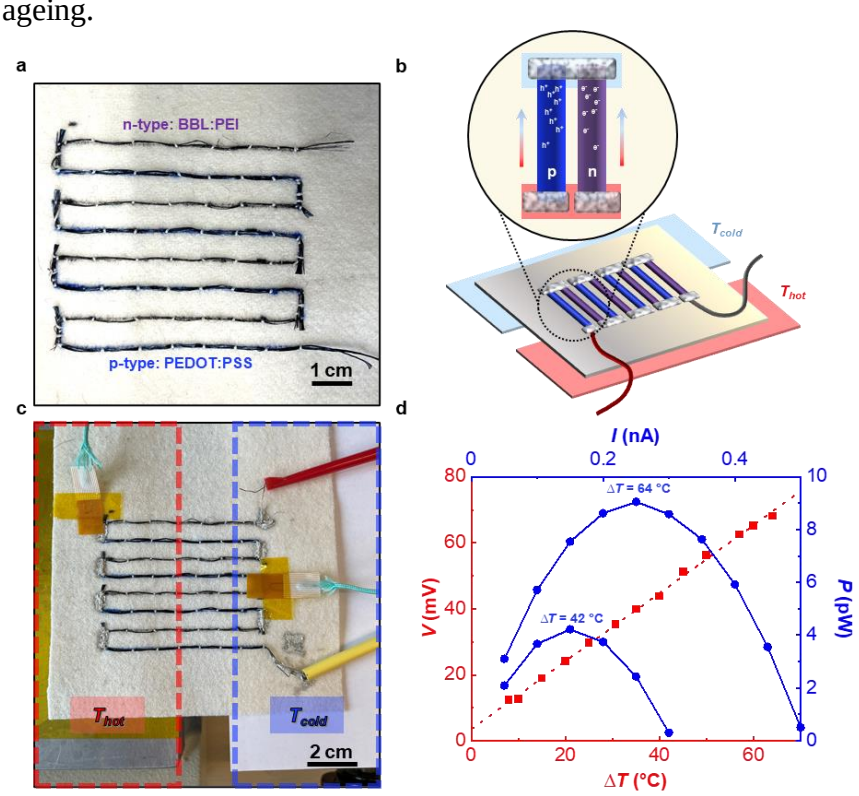

Figure 9.5. a) An in-plane thermoelectric textile generator stitched onto a felted wool fabric using BBL:PEI/SIS coated cellulose yarn (three yarns per n-type leg) and a PEDOT:PSS coated cellulose yarn (two yarns per p-type leg) that together form four n/p thermocouples. b) Schematic showing a close-up of a single thermocouple with the blue yarn representing the p-type PEDOT:PSS coated yarn while the purple yarn represents the n-type BBL:PEI/SIS coated yarn. The light blue area illustrates the heat sink (cold side) while the red area represents the heat source (hot side). c) The thermoelectric textile generator with the four n/p thermocouples electrically connected with stretchable silver paint and placed onto a heating source at temperature T_{hot} (red) and a cold side that was kept at ambient temperature T_{cold} (blue). d) The recorded open-circuit voltage V_{oc} measured for different temperature gradients $\Delta T = T_{hot} - T_{cold}$ (red) with the output power P as a function of load current I_{load} at ΔT = 42 °C or 64 °C (blue). Reprinted with permission from ref [124]. Copyright 2023 Advanced Electronic Materials published by Wiley-VCH GmbH.

With the challenge surrounding the air-stability of polymer-based n-type yarns, it was important to evaluate the ambient stability of the polymer-based textile thermoelectric devices, which included n-type polymer-based yarns (see Chapter 8). The ambient stability was not evaluated for the other thermoelectric devices from Paper I – III, which used yarns containing silver as opposed to a n-type polymer-based yarn. The thermoelectric performance of the device composed of BBL:PEI/SIS and PEDOT:PSS + EG coated yarns was monitored for several days, and the characterization was done at ambient conditions. The textile device was stored in a glovebox between measurements. After four days $V_{oc}/\Delta T$ had changed from 1.0 to 1.1 mV °C^{-1} and the maximum power output had decreased from 4.2 to 3.5 pW at ΔT = 42 °C (Figure 9.6). Evidently, polymer-based n-type yarns have potential for the realization of robust and stable thermoelectric textile devices. It can be anticipated that Paper IV will stimulate further studies into conducting polymer-based n-type yarns with higher conductivity.

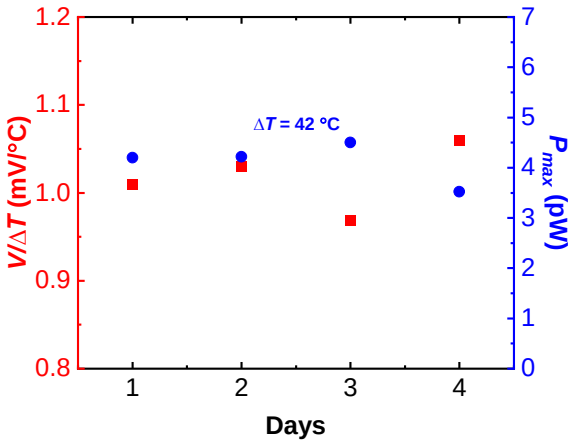

Figure 9.6. The slope of $V/\Delta T$ (red) and the output power (blue) at ΔT = 42 °C for the thermoelectric generator as a function of time. Reprinted with permission from ref [124]. Copyright 2023 Advanced Electronic Materials published by Wiley-VCH GmbH.

10. Sustainability of E-textiles

10.1. Textile and Electronic Waste

Electronics and textiles are both mass-consumer goods, which are typically used for a few years before being discarded. Electronic waste commonly consists of materials that can be valuable but challenging to salvage.[140] Occasionally, the products may contain toxic and hazardous elements, like cadmium and lead, that can be harmful if released to the environment.[11, 140] Generally, electronic waste is exceedingly varied and thus regarded as a complex waste stream. The variation can be ascribed to the tremendous amounts of products that are commercially available, which all comprise diverse materials. Alternatives to traditional electronics are consequently being explored with *green electronics*, which refers to an alternative type of electronics that solely consists of benign, i.e., non-toxic materials.[11]

For textiles, the ambition is to achieve circularity by maximizing the use of the material and products as practically feasible.[4] Textile recycling can be performed with fabrics, yarns, and fibers. For the fabrics, recycling can be achieved through cutting and re-sewing the fabric, which avoids compromising the fibers. Further, yarns can be unraveled and employed to generate other products. Recycling of textile fibers can be implemented by shredding and reprocessing. In addition, polymer recycling can be accomplished through melting or dissolving the fiber material, which can subsequently be used again.[4, 141]

Köhler et al. proposed that a combination of electronics and textile products could heighten product obsolescence. Further, it was suggested that e-textiles will generate mass products with short service lives, which would be expected to give rise to an extensive new waste stream with additional disposal and recycling challenges.[140] However, the use of e-textiles, for the fabrication of wearable electronics, has the capability of significantly improving the quality of life for people when employed for health monitoring applications.[9]

10.2. Electrically Conducting Yarns and E-textiles

Upon designing new products, one should reflect on if the components or its precursors are toxic or scarce.[4] E-textiles that use toxic materials and solvents will put the user of the material at risk in addition to the workers at the production and recycling facilities.[8] The potential consequences of the manufacturing method should be considered as well as material durability upon use.[4] Consequently, the evaluation of e-textiles for a long period of time and in various environments is of interest.[9]

Components can be reused in some instances. However, the many materials within a product can be challenging to separate. For recycling purposes, efficient methods for separating

products into components should thus be considered. An alternative could be to restrict the materials that are combined when producing e-textile. Upon separation, the conducting component that was used to fabricate the e-textile should maintain its electrical properties.[8]

10.3. Conducting Polymer and Regenerated Cellulose Yarns

Electrically conducting yarns were produced in order to fabricate e-textile devices from the bottom-up. The conducting yarns were made by using biobased substrates such as regenerated cellulose yarns, which were sourced from wood, or silk yarns instead of synthetic yarns that typically depend on fossil resources. Cotton fibers, which are also cellulose based, were not selected as a substrate yarn since the cotton crop requires considerable amounts of fresh water, pesticides and fertilizer for its cultivation.[28, 29, 47]

Specifically, regenerated cellulose yarns made by the Ioncell-F process were chosen in comparison to the viscose and the NMMO-based Lyocell process, which can result in toxic by-products, needs high temperatures and requires the use of stabilizers to avoid runaway reactions (See Chapter 4).[19, 41, 57] The ionic liquid used in the Ioncell-F process as the direct cellulose solvent is [DBNH][OAc].[19] Ionic liquids can be expensive, and some are toxic. These should consequently be recovered and recycled. Parviainen et al. evaluated the recyclability of [DBNH][OAc] with a laboratory scale trial and found that the ionic liquid could be recycled with an average recovery rate of 95.6 wt%.[142]

In this thesis, electrically conducting yarns were produced mainly by coating a substrate yarn with a conducting material. Organic semiconductors including conjugated polymers are promising materials that can be used as the conducting component for the development of e-textiles, since conjugated polymers are based on abundant elements and can in some instances be biocompatible.[10, 13] The produced conducting yarns were coated mainly with either PEDOT:PSS or BBL:PEI. PEDOT:PSS displays a promising level of biocompatibility and is thus an interesting choice.[12, 24] The n-type BBL:PEI ink was processed with ethanol unlike other n-type conducting polymers that typically require harmful halogenated solvents.[26]

The produced PEDOT: PSS coated cellulose yarns showed a promising degree of durability in the form of electrical stability upon bending, washing and at ambient conditions. The durability of the conducting yarn can extend the use of e-textile devices. For future development, it would be interesting to limit the number of different materials used for fabricating conducting yarns in addition to explore recycling of the coating layer and substrate yarn.

11. Conclusion and Outlook

Several strategies were explored in this thesis for the development of electrically conducting yarns, their characterization and for the fabrication of thermoelectric devices. The conducting yarns were produced with various combinations of conducting, semiconducting and insulating materials. To facilitate use of conducting yarns in wearable electronics, it is important to employ materials that are lightweight, benign, and scalable. Consequently, regenerated cellulose yarns and conducting polymers were used for the fabrication of conducting yarns. When considering textile polymer-based thermoelectric generators, both n-type and p-type polymer-based yarns are necessary for the fabrication of a thermoelectric generator.

To begin with, p-type PEDOT:PSS + EG coated cellulose yarns were produced with a roll-to-roll coating process, which showed, for cellulose yarn, a record-high bulk conductivity of 36 S cm^{-1}. Coated cellulose yarns displayed resilience to wash/wear and the yarns could also be used as the active material in an organic electrochemical transistor. The mechanical durability was also illustrated by machine sewing the yarns into a substrate fabric for the manufacture of an out-of-plane thermoelectric textile device that generated a power of 0.2 μW when experiencing a temperature difference of 37 K. Moreover, attempts were made to improve the durability of PEDOT:PSS + EG coated yarns by changing the substrate yarns to composite yarns of cellulose/chitosan, which, however, showed no significant improvement in washability. In addition, the roll-to-roll process was utilized to coat silk yarns, which were embroidered into a fabric and used as the p-type legs for a textile thermoelectric device.

Furthermore, regenerated cellulose yarn was coated with silver nanowires and PEDOT:PSS + EG through a dip-coating procedure and the obtained conductivity was 181 S cm^{-1}. This method was developed initially to generate PEDOT:PSS + EG/silver nanowire coated silk yarns that showed excellent durability during washing as well as a conductivity of ~320 S cm^{-1}. High conductivity values are obtained with the addition of silver nanowires to the yarn coating. Based on these results, it would be of interest to explore the possibility of using the PEDOT:PSS + EG/silver coated yarns for the fabrication of thermoelectric devices, e.g. to electrically connect p- and n-type yarns instead of applying silver paint. Thus, it would be possible to produce a thermoelectric generator where every component is yarn based, which could increase the comfortability of the device for wearable applications.

There is a lack of reported polymer-based n-type yarns. However, other types of n-type yarns have been reported that use carbon nanomaterials. There are environmental and health concerns associated with the use of carbon nanomaterials. A polymer-based n-type yarn was obtained by spray-coating regenerated cellulose yarn with BBL:PEI ink. An electrical conductivity of 8×10^{-3} S cm^{-1} was measured and the Seebeck coefficient was -79 μV K^{-1}. The electrical stability at ambient conditions was enhanced with the addition of an insulating elastomeric SIS layer to the BBL:PEI coated yarn. The n-type BBL:PEI/SIS coated cellulose yarn was used together with the p-type PEDOT:PSS coated cellulose yarn for the fabrication of a polymer-based textile thermoelectric device. The produced in-plane device showed a stable performance for at least four days, with an open-circuit voltage of about 1 mV per ºC of temperature difference. The promising stability results can be anticipated to prompt further research into the fabrication of conductive polymer-based n-type yarns.

The ambition for future development should be to explore the sustainability of e-textile materials. The evaluation can be executed at different stages of production. When considering the coating material, toxicity should be investigated for using nanomaterials on textiles that are meant to be in close skin contact with the device user. Additionally, non-toxic solvents for increasing the PEDOT:PSS conductivity should be explored. Moreover, the evaluation of the washability of conducting yarns should be continued by changing the coating formulation and the surface properties of the cellulose substrate. The washability of entire e-textile devices would also be of interest. In addition, separation strategies of the polymer-based conducting cellulose yarns into its individual components would be important to investigate with regard to material recycling.

ACKNOWLEDGEMENTS

I would like to start by thanking my supervisor Christian Müller. Thank you for giving me this opportunity to pursue a PhD and for having my back throughout this journey. I thank my co-supervisors Anja Lund and Mahiar Max Hamedi for your support.

I would like to thank all my friends and colleagues at Chalmers. Thank you for the encouragement, knowledge, laughs and for always being generous with your time. A special shoutout to the lovely people on floor 8 and the Müller group. Thank you Mariza for your kindness, Lidiya for the great chats and thanks Monika for the hugs. Thanks Sarah for nerding out with me, thanks Anders for being amazing and finally, thank you Lotta for everything that you do!

Thank you to Zijin, Zerui and Yingwei for making our office the best office in the chemistry building! You are all the sweetest people and I'm thankful that I got to spend so much time with you. Yingwei, please do not ever stop sending me funny memes.

Thank you to all my WWSC friends especially, Kenneth, Ehsan, Robin and Roujin. Thank you again Roujin for being a tremendous friend. I am lucky to know you and I'm looking forward to all our upcoming adventures.

I would also like to thank my girls Katrin, Victoria and Sandra for our sisterhood. As we approach 10 years of friendship, I look back on who we were and who we have grown into with such pride. You all are amazing and I'm so happy that I have you in my corner.

I would like to thank my friends Liam and Mate for all the fun times and great discussions.

Thank you to my platonic soulmate Paul! I don't even need to say anything because you already know. Nonetheless, thank you for lifting me up and for always being there no matter the distance.

Special thanks my mom (Haydeh), dad (Gobad), sister (Solmaz), brother-in-law (Carl) and niece (Hailey) for your endless love and support. I am nothing without you and my love for you has no bounds. Thank you for always believing in me!

Finally, I would like to thank someone who will not have the opportunity to read this, my dearest aunt (khale) Nahid. Thank you for your love and encouragement. You are terribly missed khale joon.

Sozan

BIBLIOGRAPHY

1. S. Takamatsu, T. Lonjaret, D. Crisp, J.-M. Badier, G. G. Malliaras and E. Ismailova, *Sci. Rep.*, 2015, **5**, 15003.

2. Z. Li, S. K. Sinha, G. M. Treich, Y. Wang, Q. Yang, A. A. Deshmukh, G. A. Sotzing and Y. Cao, *J. Mater. Chem. C*, 2020, **8**, 5662-5667.

3. L. Atzori, A. Iera and G. Morabito, *Comput. Netw.*, 2010, **54**, 2787-2805.

4. A. Lund, N. M. van der Velden, N.-K. Persson, M. M. Hamedi and C. Müller, *Mater. Sci. Eng., R*, 2018, **126**, 1-29.

5. Z. Tang, D. Yao, D. Du and J. Ouyang, *J. Mater. Chem. C*, 2020, **8**, 2741-2748.

6. G. Rajan, J. J. Morgan, C. Murphy, E. Torres Alonso, J. Wade, A. K. Ott, S. Russo, H. Alves, M. F. Craciun and A. I. S. Neves, *ACS Appl. Mater. Interfaces*, 2020, **12**, 29861-29867.

7. G. Chen, X. Xiao, X. Zhao, T. Tat, M. Bick and J. Chen, *Chem. Rev.*, 2022, **122**, 3259-3291.

8. A. Lund, Y. Wu, B. Fenech-Salerno, F. Torrisi, T. B. Carmichael and C. Müller, *MRS Bull.*, 2021, **46**, 491-501.

9. Y. Wu, S. S. Mechael and T. B. Carmichael, *Acc. Chem. Res.*, 2021, **54**, 4051-4064.

10. M. Irimia-Vladu, *Chem. Soc. Rev.*, 2014, **43**, 588-610.

11. M. J. Tan, C. Owh, P. L. Chee, A. K. K. Kyaw, D. Kai and X. J. Loh, *J. Mater. Chem. C*, 2016, **4**, 5531-5558.

12. M. Irimia-Vladu, E. D. Głowacki, G. Voss, S. Bauer and N. S. Sariciftci, *Mater. Today*, 2012, **15**, 340-346.

13. R. Kroon, D. A. Mengistie, D. Kiefer, J. Hynynen, J. D. Ryan, L. Yu and C. Müller, *Chem. Soc. Rev.*, 2016, **45**, 6147-6164.

14. A. Giovannitti, C. B. Nielsen, D.-T. Sbircea, S. Inal, M. Donahue, M. R. Niazi, D. A. Hanifi, A. Amassian, G. G. Malliaras, J. Rivnay and I. McCulloch, *Nat. Commun.*, 2016, **7**, 13066.

15. S. Agate, M. Joyce, L. Lucia and L. Pal, *Carbohydr. Polym.*, 2018, **198**, 249-260.

16. F. Hoeng, A. Denneulin and J. Bras, *Nanoscale*, 2016, **8**, 13131-13154.

17. M. Jabbar and K. Shaker, in *Textile Engineering - An Introduction*, ed. Y. Nawab, Berlin, Boston, Berlin, Boston, 2016, DOI: doi:10.1515/9783110413267-004, pp. 7-24.

18. R. R. Mather and R. H. Wardman, in *Chemistry of Textile Fibres (2nd Edition)*, Royal Society of Chemistry (RSC), 2016.

19. H. Sixta, A. Michud, L. Hauru, S. Asaadi, Y. Ma, A. W. T. King, I. Kilpeläinen and M. Hummel, *Nord. Pulp Pap. Res. J.*, 2015, **30**, 43-57.

20. Y. Ma, M. Hummel, M. Määttänen, A. Särkilahti, A. Harlin and H. Sixta, *Green Chem.*, 2016, **18**, 858-866.

21. R. Sarabia-Riquelme, R. Andrews, J. E. Anthony and M. C. Weisenberger, *J. Mater. Chem. C*, 2020, **8**, 11618-11630.

22. S. Timpanaro, M. Kemerink, F. J. Touwslager, M. M. De Kok and S. Schrader, *Chem. Phys. Lett.*, 2004, **394**, 339-343.

23. N. Kim, S. Kee, S. H. Lee, B. H. Lee, Y. H. Kahng, Y.-R. Jo, B.-J. Kim and K. Lee, *Adv. Mater.*, 2014, **26**, 2268-2272.

24. M. Asplund, E. Thaning, J. Lundberg, A. C. Sandberg-Nordqvist, B. Kostyszyn, O. Inganäs and H. von Holst, *Biomed. Mater.*, 2009, **4**, 045009.

25. J. D. Ryan, D. A. Mengistie, R. Gabrielsson, A. Lund and C. Müller, *ACS Appl. Mater. Interfaces*, 2017, **9**, 9045-9050.

26. C.-Y. Yang, M.-A. Stoeckel, T.-P. Ruoko, H.-Y. Wu, X. Liu, N. B. Kolhe, Z. Wu, Y. Puttisong, C. Musumeci, M. Massetti, H. Sun, K. Xu, D. Tu, W. M. Chen, H. Y. Woo, M. Fahlman, S. A. Jenekhe, M. Berggren and S. Fabiano, *Nat. Commun.*, 2021, **12**, 2354.

27. R. R. Mather and R. H. Wardman, in *Chemistry of Textile Fibres*, Royal Society of Chemistry, 2011.

28. G. Sandin, S. Roos and M. Johansson, *Environmental impact of textile fibers – what we know and what we don't know : Fiber Bible part 2*, Report 978-91-88695-91-8 (ISBN), Göteborg, 2019.

29. M. Bevilacqua, F. E. Ciarapica, G. Mazzuto and C. Paciarotti, *J. Cleaner Prod.*, 2014, **82**, 154-165.

30. FAO, *Building a Common Vision for Sustainable Food and Agriculture. Principles and Approaches*, Report ISBN 978-92-5-108471-7, Rome, 2014.

31. Z. Ali, in *Textile Engineering - An Introduction*, ed. Y. Nawab, De Gruyter Oldenbourg, Berlin, Boston, 2016, DOI: doi:10.1515/9783110413267-005, pp. 25-46.

32. R. Alagirusamy and A. Das, in *Textiles and Fashion*, ed. R. Sinclair, Woodhead Publishing, 2015, DOI: https://doi.org/10.1016/B978-1-84569-931-4.00008-8, pp. 159-189.

33. Y. E. Elmogahzy, in *Engineering Textiles - Integrating the Design and Manufacture of Textile Products (2nd Edition)*, Elsevier, 2020, pp. 223-248.

34. E. Britannica, knitting machine, https://www.britannica.com/technology/knitting-machine, (accessed 2023-01-11).

35. D. J. Spencer, in *Knitting Technology - A Comprehensive Handbook and Practical Guide (3rd Edition)*, Woodhead Publishing, 2001.

36. T. Hussain, in *Textile Engineering - An Introduction*, ed. Y. Nawab, De Gruyter Oldenbourg, Berlin, Boston, 2016, DOI: doi:10.1515/9783110413267-007, pp. 83-110.

37. A. C. O'Sullivan, *Cellulose*, 1997, **4**, 173-207.

38. C. Brigham, in *Green Chemistry*, eds. B. Török and T. Dransfield, Elsevier, 2018, DOI: https://doi.org/10.1016/B978-0-12-809270-5.00027-3, pp. 753-770.

39. K. L. Yam, in *Wiley Encyclopedia of Packaging Technology (3rd Edition)*, John Wiley & Sons, 2019, p. 111.

40. K. H. J. Buschow, R. W. Cahn, M. C. Flemings, B. Ilschner, E. J. Kramer and S. Mahajan, in *Encyclopedia of Materials - Science and Technology, Volumes 1-11*, Elsevier, 2001.

41. A. Michud, Aalto University, 2016.

42. M. M. Mahmud, A. Perveen, R. A. Jahan, M. A. Matin, S. Y. Wong, X. Li and M. T. Arafat, *Int. J. Biol. Macromol.*, 2019, **130**, 969-976.

43. E. Jin, J. Guo, F. Yang, Y. Zhu, J. Song, Y. Jin and O. J. Rojas, *Carbohydr. Polym.*, 2016, **143**, 327-335.

44. T. Rosén, B. S. Hsiao and L. D. Söderberg, *Adv. Mater.*, 2020, **n/a**, 2001238.

45. T. Nishino, K. Takano and K. Nakamae, *J. Polym. Sci., Part B: Polym. Phys.*, 1995, **33**, 1647-1651.

46. J. Zhang, J. Wu, J. Yu, X. Zhang, J. He and J. Zhang, *Mater. Chem. Front.*, 2017, **1**, 1273-1290.

47. C. Olsson and G. Westman, *J. Appl. Polym. Sci.*, 2013, **127**, 4542-4548.

48. S. Zhu, Y. Wu, Q. Chen, Z. Yu, C. Wang, S. Jin, Y. Ding and G. Wu, *Green Chem.*, 2006, **8**, 325-327.

49. B. Thomas, M. C. Raj, A. K. B, R. M. H, J. Joy, A. Moores, G. L. Drisko and C. Sanchez, *Chem. Rev.*, 2018, **118**, 11575-11625.

50. R. J. Moon, *McGraw-Hill Yearbook of Science and Technology*, 2008.

51. C. Chen and L. Hu, *Adv. Mater.*, 2021, **33**, 2002890.

52. C. Chen, Y. Kuang, S. Zhu, I. Burgert, T. Keplinger, A. Gong, T. Li, L. Berglund, S. J. Eichhorn and L. Hu, *Nat. Rev. Mater.*, 2020, **5**, 642-666.

53. R. K. Gond, M. K. Gupta, H. Singh, S. Mavinkere Rangappa and S. Siengchin, in *Biodegradable Polymers, Blends and Composites*, eds. S. M. Rangappa, J. Parameswaranpillai, S. Siengchin and M. Ramesh, Elsevier, 2022, pp. 59-86.

54. N. Mittal, *Nanostructured Biopolymeric Materials: Hydrodynamic Assembly, Mechanical Properties and Bio-Functionalities*, KTH Royal Institute of Technology, 2019.

55. Y. E. Elmogahzy, in *Engineering Textiles - Integrating the Design and Manufacture of Textile Products (2nd Edition)*, Elsevier, 2019.

56. J. Chen, in *Textiles and Fashion*, ed. R. Sinclair, Woodhead Publishing, 2015, DOI: https://doi.org/10.1016/B978-1-84569-931-4.00004-0, pp. 79-95.

57. T. Liebert, in *Cellulose Solvents: For Analysis, Shaping and Chemical Modification*, American Chemical Society, 2010, vol. 1033, ch. 1, pp. 3-54.

58. B. Ozipek and H. Karakas, in *Advances in Filament Yarn Spinning of Textiles and Polymers*, ed. D. Zhang, Woodhead Publishing, 2014, DOI: https://doi.org/10.1533/9780857099174.2.174, pp. 174-186.

59. S. Asaadi, DOI: 10.13140/RG.2.2.22801.79205, 2019.

60. T. Rosenau, A. Potthast, H. Sixta and P. Kosma, *Prog. Polym. Sci.*, 2001, **26**, 1763-1837.

61. A. Michud, M. Tanttu, S. Asaadi, Y. Ma, E. Netti, P. Kääriainen, A. Persson, A. Berntsson, M. Hummel and H. Sixta, *Text. Res. J.*, 2016, **86**, 543-552.

62. S. J. Haward, V. Sharma, C. P. Butts, G. H. McKinley and S. S. Rahatekar, *Biomacromolecules*, 2012, **13**, 1688-1699.

63. Encyclopedia Britannica, sliver, https://www.britannica.com/technology/sliver, (accessed 2022-12-07).

64. R. Chattopadhyay, in *Technical Textile Yarns - Industrial and Medical Applications*, eds. R. Alagirusamy and A. Das, Woodhead Publishing, 2010, pp. 3-55.

65. F. Carpi and D. D. Rossi, *IEEE trans. inf. technol. biomed.*, 2005, **9**, 295-318.

66. F. Jiao, in *Flexible and Wearable Electronics for Smart Clothing*, eds. G. Wang, C. Hou and H. Wang, John Wiley & Sons, 2020, DOI: https://doi.org/10.1002/9783527818556.ch3, pp. 49-66.

67. J. D. Ryan, A. Lund, A. I. Hofmann, R. Kroon, R. Sarabia-Riquelme, M. C. Weisenberger and C. Müller, *ACS Appl. Energy Mater.*, 2018, **1**, 2934-2941.

68. A. Lund, K. Rundqvist, E. Nilsson, L. Yu, B. Hagström and C. Müller, *npj Flexible Electron.*, 2018, **2**, 1-9.

69. J. Chen, Y. Huang, N. Zhang, H. Zou, R. Liu, C. Tao, X. Fan and Z. L. Wang, *Nat. Energy*, 2016, **1**, 16138.

70. M. Hatamvand, E. Kamrani, M. Lira-Cantú, M. Madsen, B. R. Patil, P. Vivo, M. S. Mehmood, A. Numan, I. Ahmed and Y. Zhan, *Nano Energy*, 2020, **71**, 104609.

71. X. Pu, L. Li, H. Song, C. Du, Z. Zhao, C. Jiang, G. Cao, W. Hu and Z. L. Wang, *Adv. Mater.*, 2015, **27**, 2472-2478.

72. B. Wang and A. Facchetti, in *Flexible and Wearable Electronics for Smart Clothing*, eds. G. Wang, C. Hou and H. Wang, John Wiley & Sons, 2020, DOI: https://doi.org/10.1002/9783527818556.ch13, pp. 305-334.

73. K. Kirihara, Q. Wei, M. Mukaida and T. Ishida, *Synth. Met.*, 2017, **225**, 41-48.

74. Y. Atwa, N. Maheshwari and I. A. Goldthorpe, *J. Mater. Chem. C*, 2015, **3**, 3908-3912.

75. K. Klinkhammer, R. Nolden, R. Brendgen, M. Niemeyer, K. Zöll and A. Schwarz-Pfeiffer, *Polymers*, 2022, **14**, 806.

76. ChemSec, SIN List, https://sinsearch.chemsec.org/chemical/308068-56-6, (accessed 2021-10-04, 2020).

77. A. M. Grancarić, I. Jerković, V. Koncar, C. Cochrane, F. M. Kelly, D. Soulat and X. Legrand, *J. Ind. Text.*, 2018, **48**, 612-642.

78. S. Nature, Conjugated polymers, https://www.nature.com/subjects/conjugated-polymers, (accessed 2022-12-20).

79. A. I. Hofmann, R. Kroon and C. Müller, in *Handbook of Organic Materials for Electronic and Photonic Devices (Second Edition)*, ed. O. Ostroverkhova, Woodhead Publishing, 2019, DOI: https://doi.org/10.1016/B978-0-08-102284-9.00013-9, pp. 429-449.

80. G. Kaur, R. Adhikari, P. Cass, M. Bown and P. Gunatillake, *RSC Adv.*, 2015, **5**, 37553-37567.

81. I. Petsagkourakis, N. Kim, K. Tybrandt, I. Zozoulenko and X. Crispin, *Adv. Electron. Mater.*, 2019, **5**, 1800918.

82. J. Rivnay, S. Inal, B. A. Collins, M. Sessolo, E. Stavrinidou, X. Strakosas, C. Tassone, D. M. Delongchamp and G. G. Malliaras, *Nat. Commun.*, 2016, **7**, 11287.

83. M. Berggren, X. Crispin, S. Fabiano, M. P. Jonsson, D. T. Simon, E. Stavrinidou, K. Tybrandt and I. Zozoulenko, *Adv. Mater.*, 2019, **31**, 1805813.

84. C. Müller, L. Ouyang, A. Lund, K. Moth-Poulsen and M. M. Hamedi, *Adv. Mater.*, 2019, **31**, 1807286.

85. M. Hamedi, R. Forchheimer and O. Inganäs, *Nat. Mater.*, 2007, **6**, 357-362.

86. J. A. Lee, A. E. Aliev, J. S. Bykova, M. J. de Andrade, D. Kim, H. J. Sim, X. Lepró, A. A. Zakhidov, J.-B. Lee, G. M. Spinks, S. Roth, S. J. Kim and R. H. Baughman, *Adv. Mater.*, 2016, **28**, 5038-5044.

87. A. Bar-Cohen, in *Encyclopedia of Thermal Packaging (Set 1) Thermal Packaging Techniques, Volumes 1-6*, World Scientific, 2012.

88. N. Komatsu, Y. Ichinose, O. S. Dewey, L. W. Taylor, M. A. Trafford, Y. Yomogida, G. Wehmeyer, M. Pasquali, K. Yanagi and J. Kono, *Nat. Commun.*, 2021, **12**, 4931.

89. M. Ito, T. Koizumi, H. Kojima, T. Saito and M. Nakamura, *J. Mater. Chem. A*, 2017, **5**, 12068-12072.

90. J. Liu, G. Liu, J. Xu, C. Liu, W. Zhou, P. Liu, G. Nie, X. Duan and F. Jiang, *ACS Appl. Energy Mater.*, 2020, **3**, 6165-6171.

91. Y. Lin, J. Liu, X. Wang, J. Xu, P. Liu, G. Nie, C. Liu and F. Jiang, *Compos. Commun.*, 2019, **16**, 79-83.

92. J. Pope and C. Lekakou, *Smart Mater. Struct.*, 2019, **28**, 095006.

93. X. Lan, T. Wang, C. Liu, P. Liu, J. Xu, X. Liu, Y. Du and F. Jiang, *Compos. Sci. Technol.*, 2019, **182**, 107767.

94. A. Lund, S. Darabi, S. Hultmark, J. D. Ryan, B. Andersson, A. Ström and C. Müller, *Adv. Mater. Technol.*, 2018, **3**, 1800251.

95. T. Bashir, M. Skrifvars and N.-K. Persson, *Polym. Adv. Technol.*, 2011, **22**, 2214-2221.

96. S. S. Rahatekar, A. Rasheed, R. Jain, M. Zammarano, K. K. Koziol, A. H. Windle, J. W. Gilman and S. Kumar, *Polymer*, 2009, **50**, 4577-4583.

97. J. Choi, Y. Jung, S. J. Yang, J. Y. Oh, J. Oh, K. Jo, J. G. Son, S. E. Moon, C. R. Park and H. Kim, *ACS Nano*, 2017, **11**, 7608-7614.

98. R. R. Mather and R. H. Wardman, in *Chemistry of Textile Fibres*, Royal Society of Chemistry, 2011.

99. D. N. Rockwood, R. C. Preda, T. Yücel, X. Wang, M. L. Lovett and D. L. Kaplan, *Nat. Protoc.*, 2011, **6**, 1612-1631.

100. Y. Kim, A. Lund, H. Noh, A. I. Hofmann, M. Craighero, S. Darabi, S. Zokaei, J. I. Park, M. H. Yoon and C. Müller, *Macromol. Mater. Eng.*, 2020, **305**, 1900749.

101. H. Okuzaki, Y. Harashina and H. Yan, *Eur. Polym. J.*, 2009, **45**, 256-261.

102. S. Iwamoto, A. Isogai and T. Iwata, *Biomacromolecules*, 2011, **12**, 831-836.

103. Y. Kim, A. Lund, H. Noh, A. I. Hofmann, M. Craighero, S. Darabi, S. Zokaei, J. I. Park, M.-H. Yoon and C. Müller, *Macromolecular Materials and Engineering*, 2020, **305**, 1900749.

104. A. B. Fall, F. Hagel, J. Edberg, A. Malti, P. A. Larsson, L. Wågberg, H. Granberg and K. M. O. Håkansson, *ACS Appl. Polym. Mater.*, 2022, **4**, 4119-4130.

105. A. International, ASTM D4966-12(2016) Standard Test Method for Abrasion Resistance of Textile Fabrics (Martindale Abrasion Tester Method), https://www.astm.org/d4966-12r16.html, (accessed 2022-12-10).

106. I. O. f. Standardization, ISO 7854:1995 Rubber- or plastics-coated fabrics — Determination of resistance to damage by flexing, https://www.iso.org/standard/14777.html, (accessed 2022-12-11).

107. R. N. Wright, in *Wire Technology - Process Engineering and Metallurgy (2nd Edition)*, Elsevier, 2016.

108. J. Pionteck and G. Wypych, in *Handbook of Antistatics (2nd Edition)*, ChemTec Publishing, 2016.

109. M. Wang, in *Understandable Electric Circuits - Key Concepts (2nd Edition)*, Institution of Engineering and Technology (The IET), 2019.

110. V. Šafářová, L. Hes and J. Militký, 2014.

111. J. D. Ryan, Chalmers University of Technology, 2018.

112. G. Windred, *J. Franklin Inst.*, 1941, **231**, 547-585.

113. C. Zhai, D. Hanaor, G. Proust, L. Brassart and Y. Gan, *Extreme Mech. Lett.*, 2016, **9**, 422-429.

114. F. K. Ko and Y. Wan, in *Introduction to Nanofiber Materials*, Cambridge University Press, 2014.

115. S. W. Beckwith, K. M. Storage, T. M. Storage and N. Titchenal, in *SAMPE 2013 - Education & Green Sky - Materials Technology for a Better World, Long Beach, CA, May 06-09, 2013*, Society for the Advancement of Material and Process Engineering (SAMPE), 2013.

116. A. P. Schuetze, W. Lewis, C. Brown and W. J. Geerts, *Am. J. Phys.*, 2004, **72**, 149-153.

117. T. Bashir, L. Fast, M. Skrifvars and N.-K. Persson, *J. Appl. Polym. Sci.*, 2012, **124**, 2954-2961.

118. G. K. Reeves and H. B. Harrison, *IEEE Electron Device Lett.*, 1982, **3**, 111-113.

119. S. Darabi, M. Hummel, S. Rantasalo, M. Rissanen, I. Öberg Månsson, H. Hilke, B. Hwang, M. Skrifvars, M. M. Hamedi, H. Sixta, A. Lund and C. Müller, *ACS Appl. Mater. Interfaces*, 2020, **12**, 56403-56412.

120. Y. H. Kim, C. Sachse, M. L. Machala, C. May, L. Müller-Meskamp and K. Leo, *Adv. Funct. Mater.*, 2011, **21**, 1076-1081.

121. D. Alemu Mengistie, P.-C. Wang and C.-W. Chu, *J. Mater. Chem. C*, 2013, **1**, 9907-9915.

122. D. Alemu Mengistie, H.-Y. Wei, K.-C. Ho and C.-W. Chu, *Energy Environ. Sci.*, 2012, **5**, 9662-9671.

123. A. M. Nardes, M. Kemerink, M. M. de Kok, E. Vinken, K. Maturova and R. A. J. Janssen, *Org. Electron.*, 2008, **9**, 727-734.

124. S. Darabi, C.-Y. Yang, Z. Li, J.-D. Huang, M. Hummel, H. Sixta, S. Fabiano and C. Müller, *Adv. Electron. Mater.*, 2023.

125. A. Savva, S. Wustoni and S. Inal, *J. Mater. Chem. C*, 2018, **6**, 12023-12030.

126. C. Müller, M. Hamedi, R. Karlsson, R. Jansson, R. Marcilla, M. Hedhammar and O. Inganäs, *Adv. Mater.*, 2011, **23**, 898-901.

127. J. M. G. Cowie,

Arrighi, V, *Polymers: Chemistry and Physics of Modern Materials*, CRC Press, Boca Raton, 3rd Edition edn., 2007.

128. P. A. Tres, in *Designing Plastic Parts for Assembly (9th Edition)*, Hanser Publishers, 2014.

129. M. A. Spalding and A. M. Chatterjee, in *Handbook of Industrial Polyethylene and Technology - Definitive Guide to Manufacturing, Properties, Processing, Applications and Markets*, John Wiley & Sons, 2018.

130. S. Burkinshaw, *Physico-chemical Aspects of Textile Coloration*, 2015.

131. A. International, ASTM WK61480 New Test Method for Durability of Smart Garment Textile Electrodes after Laundering, https://www.astm.org/workitem-wk61480, (accessed 2022-12-10).

132. I. O. f. Standardization, ISO 6330:2021 Textiles — Domestic washing and drying procedures for textile testing, https://www.iso.org/obp/ui#iso:std:iso:6330:ed-4:v1:en (accessed 2022-12-11).

133. N. Massonnet, A. Carella, O. Jaudouin, P. Rannou, G. Laval, C. Celle and J.-P. Simonato, *J. Mater. Chem. C*, 2014, **2**, 1278-1283.

134. H. Zahra, D. Sawada, C. Guizani, Y. Ma, S. Kumagai, T. Yoshioka, H. Sixta and M. Hummel, *Biomacromolecules*, 2020, **21**, 4326-4335.

135. J. A. Sirviö, A. M. Kantola, S. Komulainen and S. Filonenko, *Biomacromolecules*, 2021, **22**, 2119-2128.

136. S. Beeby and N. White, in *Energy Harvesting for Autonomous Systems*, Artech House, 2010.

137. Q. Wu and J. Hu, *Smart Mater. Struct.*, 2017, **26**, 045037.

138. L. Wang and K. Zhang, *Energy Environ. Mater.*, 2020, **3**, 67-79.

139. B. Hwang, A. Lund, Y. Tian, S. Darabi and C. Müller, *ACS Appl. Mater. Interfaces*, 2020, **12**, 27537-27544.

140. A. R. Köhler, L. M. Hilty and C. Bakker, *J. Ind. Ecol.*, 2011, **15**, 496-511.

141. *A New Textiles Economy: Redesigning fashion's future*, The Ellen MacArthur Foundation, 2017.

142. A. Parviainen, R. Wahlström, U. Liimatainen, T. Liitiä, S. Rovio, J. K. J. Helminen, U. Hyväkkö, A. W. T. King, A. Suurnäkki and I. Kilpeläinen, *RSC Adv.*, 2015, **5**, 69728-69737.